TITLE

Changes in hydrology and erosion over a transition from grassland to shrubland

AUTHORS

Turnbull, Laura; Wainwright, John; Brazier, Richard E.

JOURNAL

Hydrological Processes

DEPOSITED IN ORE

17 June 2013

Hydrological and erosion variation over a transition from grassland to shrubland

Journal:	*Hydrological Processes*
Manuscript ID:	HYP-08-0619.R2
Wiley - Manuscript type:	Research Article
Date Submitted by the Author:	
Complete List of Authors:	Turnbull, Laura; Arizona State University, Global Institute of Sustainability Wainwright, John; University of Sheffield, Department of Geography Brazier, Richard; University of Exeter, Department of Geography
Keywords:	Runoff, Erosion, Soil moisture, Ecohydrology, Connectivity , Land degradation

Hydrological and erosion variation over a transition from grassland to shrubland

Laura Turnbull
Global Institute of Sustainability, Arizona State University, 800 South Cady Mall, POB 875402, Tempe, Arizona, 85287, USA

John Wainwright
Sheffield Centre for International Drylands Research, Department of Geography, University of Sheffield, Winter Street, Sheffield, S10 2TN, UK

Richard E Brazier
Department of Geography, University of Exeter, Amory Building, Rennes Drive, Exeter, EX4 4RJ, UK

Abstract

The degradation of grasslands is a common problem across semi-arid areas worldwide. Over the last 150 years much of the South-Western USA has experienced significant land degradation, with desert grasslands becoming dominated by shrubs and concurrent changes in runoff and erosion which are thought to propagate further the process of degradation. Plot-based experiments to determine how spatio-temporal characteristics of soil moisture, runoff and erosion change over a transition from grassland to shrubland were carried out at four sites over a transition from black grama (*Bouteloua eriopoda*) grassland to creosotebush (*Larrea tridentata*) shrubland at the Sevilleta NWR LTER site in New Mexico. Each site consisted of a 10 x 30 m bounded runoff plot and adjacent characterisation plots with nested sampling points where soil-moisture content was measured. Results show distinct spatio-temporal variations in soil-moisture content, which are due to the net effect of processes operating at multiple spatial and temporal scales, such as plant uptake of water at local scales versus the redistribution of water during runoff events at the hillslope scale. There is an overall increase in runoff and erosion over the transition from grassland to shrubland, which is likely to be associated with an increase in connectivity of bare, runoff-generating areas, although these increases do not appear to follow a linear trajectory. Erosion rates increased over the transition from grassland to shrubland, likely related in part to changes in runoff characteristics and the increased capacity of the runoff to detach, entrain and transport sediment. Over all plots fine material was preferentially eroded which has potential implications for nutrient cycling since nutrients tend to be associated with fine sediment.

Keywords:

Runoff, erosion, soil-moisture, spatial autocorrelation, ecohydrology, land degradation, connectivity, desertification

Introduction

The degradation of grasslands is a common problem across semi-arid areas worldwide. Over the last 150 years much of the South-Western USA has experienced significant land degradation, with desert grasslands becoming dominated by shrubs (Buffington and Herbel, 1965; Humphrey, 1953; 1958). The increases in runoff and erosion under shrubland vegetation (Abrahams *et al.*, 1995; Parsons *et al.*, 1996) are widespread land-degradation problems because of the resulting increased resource loss from ecosystems. In shrublands, shrubs are able to capture and retain nutrients, in accordance with the 'islands of fertility' concept (Charley and West, 1975; Schlesinger *et al.*, 1990), although the bare inter-shrub areas become increasingly degraded, which decreases the likelihood for grass re-establishment in these areas. Therefore, not only is there increased resource loss over shrublands, but also changes in the spatial distribution of remaining resources (Müller *et al.*, 2008; Schlesinger *et al.*, 1996; Turnbull *et al.*, in review). Understanding the dynamics of land degradation in terms of changes in ecosystem structure and function, including runoff and erosion, is crucial in order for sustainable land-management to be practiced, or for the process of shrub invasion of grasslands to be reversed (Turnbull *et al.*, 2008).

Semi-arid surface hydrology is determined by the interplay of surface and near-surface processes operating over a continuum of temporal and spatial scales that are dependent upon biotic and abiotic structural characteristics of the ecosystem. These hydrological processes operate at different spatial and temporal scales, yet are intimately connected as a result of interactions and feedbacks between ecosystem structure and function. For instance, soil moisture varies both spatially and temporally, and is important in understanding the biotic response in semi-arid regions and their influence on hydrologic or abiotic responses (Gosz, 1993; Huenneke and Schlesinger, 2004; Kurc and Small, 2007). Therefore, understanding patterns of soil moisture is critical in establishing models of ecosystem function (Snyder *et al.*, 2005) and in understanding and predicting the temporal and spatial hydrological response to a rainfall event. The ecological significance of a spatial pattern measured at one point in time is difficult to assess without an understanding of the temporal variability of that pattern (Gustafson, 1998). Understanding the spatio-temporal dynamics of runoff generation is particularly important because of the influence of antecedent conditions on runoff generation (Wainwright *et al.*, 2008a), the availability of moisture for plant growth and the effects of soil moisture on nutrient cycling (Wainwright, 2009).

As yet, there is little understanding of how runoff, erosion and soil moisture vary spatially and temporally when there is a transition from grassland to shrubland in the South-Western USA or in other comparable semi-arid ecosystems. To understand the dynamics of semi-arid land degradation, interactions between ecosystem structure and function need to be determined at stages during the transition from grassland to shrubland (Turnbull *et al*. 2008). Changes in the amount and spatial structure of vegetation, soil structure and resource characteristics that are likely to affect surface hydrology and erosion at stages over a transition from grassland to shrubland were evaluated by Turnbull *et al*. (in review). The aim of this paper is to investigate how inter-event (soil-moisture content) and intra-event (runoff surface hydrology and erosion) alter in response to, and in interaction with, a change in vegetation over a transition from grassland to shrubland.

The specific objectives of this paper are:

1. to determine how spatio-temporal soil-moisture dynamics change over a transition from grassland to shrubland;
2. to determine how runoff and erosion change as a result of change in ecosystem structure over a transition from grassland to shruband;
3. to determine the changes in feedbacks and linkages between structural connectivity (soil moisture) and functional connectivity (runoff and erosion) over the transition from grassland to shrubland.

Methods

Field-based monitoring was carried out at the Sevilleta National Wildlife Refuge (SNWR) in central New Mexico, USA (34°19' N, 106°42' W). Here an ecotone marks the boundary between semi-arid black grama (*Bouteloua eriopoda*) grassland and creosotebush (*Larrea tridentata*) shrubland (Gosz, 1993). Monitoring was carried out at four locations over a grassland to shrubland ecotone, on the premise that differences in processes observed over the grassland to shrubland ecotone will be equivalent to changes that occur through time during grassland to shrubland transitions (the ergodic hypothesis) (Figure 1). Due to the time-consuming and costly nature of the monitoring work undertaken, it was not possible to replicate plots at each stage over the transition. The four study sites were selected to be representative of different stages over the transition from grassland to shrubland, in terms of changes in vegetation cover, and associated changes in ecosystem structure and function (see Turnbull *et al.* 2008). Vegetation and soil characteristics of each site are detailed in Table 1.

Each of the four study sites (Figure 2) consist of a 10-m across slope by 30-m downslope runoff and erosion plot, and two 5 × 30 m characterisation plots. The latter were set up with a nested, broad and fine-scale sampling strategy for the measurement of soil-surface properties. The SNWR experiences a semi-arid climate and has a long-term mean annual precipitation averaging 256 mm (1989 – 2006), 53 % of which typically falls as intense rainfall during the summer monsoon period between July and September. A more in depth description of the study sites and SNWR is provided in Turnbull *et al.* (in review) and at Sevilleta LTER (2008).

The availability of soil moisture in time and space is the most important factor in determining the structure and dynamics of ecosystems in semi-arid regions (Noy-Meir, 1973). Soil-moisture is a complex space-time variable (Buttafuoco *et al.*, 2005). Typically, the soil in semi-arid and arid regions is dry except for brief periods following rainfall events (Bhark and Small, 2003). Therefore, in order to determine surface soil-moisture dynamics, and in particular post rainfall event soil-moisture dynamics, frequent monitoring was required. Measurements of the volumetric soil moisture content at residual air saturation (θ_s) at 90 nested sampling points on the characterization plots (i.e. either side of the runoff plot) were taken using a Delta-T ML2x Theta probe (Figure 3) which measures θ_s to a depth of 5 cm. On the grass plot, 44 of these sampling points were in bare soil and 46 in grass patches, on the grass-shrub plot 34 were in bare soil, 31 in grass patches and 25 under shrubs, in the shrub-grass plot 35 were in bare soil, 22 in grass patches and 23 under shrubs and in the shrub plot 47 were in bare soil and 43 under shrubs. Measurements were taken on a daily basis during wet periods, with a decline in the frequency of measurements to every two to three days during dry periods when variations in soil-moisture content were minimal. Geostatistical analysis of soil-moisture content was carried out calculating omnidirectional experimental variograms using GSTAT within Idrisi32. The semi-variogram was then modelled using a Gaussian model (see Turnbull *et al.* in review for further detail). The degree of spatial dependence was classified in accordance with the criteria of Cambardella *et al.* (1994) where a nugget/sill ratio less than or equal to 0.25 is considered to be strongly spatially dependent, a nugget/sill ratio between 0.25 and 0.75 is moderately spatially dependent and a nugget/sill ratio greater than 0.75 is considered to be weakly spatially dependent.

The four plots installed over the grass to shrub transition are of identical design, measuring 10 × 30 m (Figure 4). This size was used as it encompasses the key features of vegetation patchiness and inter-shrub areas, whilst still being manageable in terms of the practicalities of construction and data collection. The plots were constructed according to the design outlined in Parsons *et al.* (2006). Plots were bounded in order that inputs and outputs could be quantified. The upper and side boundaries of the plots were constructed by inserting aluminium flashing into a shallow trench dug into the soil, then buttressed by soil on the outside edge of the plot. The lower boundary of the plots were made of guttering which collected and channelled water leaving the plot through a supercritical flume, which was installed at a slope of 4 %. A tipping-bucket rain gauge was used to measure rainfall intensity at one-minute intervals. Additionally, two V-shaped collecting rain gauges were installed at the top of the plot and midway down the plot so that spatial variations in total rainfall could be assessed.

The flumes were equipped with ISCO 6700 pump samplers and ISCO 730 bubbler modules to measure the depth of runoff passing through the flumes and to collect samples of runoff leaving the plot at one minute intervals once flow depth was at or above 15 mm on the grass and grass-shrub plots, and 20 mm on the shrub-grass and shrub plots. These different depths were chosen over the plots in an attempt to sample runoff for the full duration of flow (or as near to the full duration as possible). Since runoff tends to be less over grassland (Parsons *et al.*, 1996; Wainwright *et al.*, 2000), the depth at which sampling is initiated was set to be lower over the grass and grass-shrub plots. The measured flow depth from each plot was rated against the discharge to develop an uncertain stage-discharge relationship, whereby errors inherent in the calibration (i.e. instrument errors) along both the abcissa and ordinate axes of the calibration curve were quantified, so that the discharge of runoff (with estimated error) could be determined from the measured flow depth. From the supercritical flumes, the runoff was captured in a 2120-litre galvanized stock tank, which was covered to exclude direct rainfall. Thus, scaling of the event hydrograph to the known volume of runoff measured in the stock tank was used to constrain the potential errors in the event hydrograph. Scaling the hydrograph becomes problematic for those events where the volume of runoff exceeded the capacity of the stock tanks. Therefore, hydrographs where the volume of total runoff is unknown are scaled according to the relationship derived between hydrograph Q and measured Q for the events that were measured. Relationships are derived for the upper and lower error bounds of hydrograph Q and measured Q. Since uncertainty in the relationship between hydrograph Q and measured Q increases with increases in Q, scaling the hydrographs to determine the minimum and maximum error bounds has the effect of increasing the error margins of the measured hydrographs. Recognising potential uncertainty in the flow hydrograph is important because calculation of runoff coefficients will be highly sensitive to uncertainty in the flow hydrograph, comparison of the hydrological response between events or between plots will be flawed without consideration of uncertainty in the hydrograph, and calculation of nutrient and sediment fluxes depend upon Q. Therefore errors in Q will propagate through calculations of sediment, total dissolved and particulate-bound nutrient export from the plots. Uncertainty associated with field observations is rarely quantified in the literature, though see notable exceptions in Krueger *et al*. (2009), BoixFayos *et al*. (2007) and Wainwright *et al*. (2008b). Thus, the dataset presented here represents a significant improvement when compared to the standard 'single-line' hydrographs that are typically produced.

After rainfall events, rainfall/runoff data and runoff samples were collected from the ISCO auto-sampler. To determine the total water/sediment output from the plots, the depth of water in the stock tank was measured, and the water was then pumped out using a bilge pump, with minimal disturbance to the sediment that had settled at the bottom of the stock tank. The remaining sediment in the stock tank was left to dry, and was then collected for subsequent analysis. Sediment from the gutters and flume was also collected and added to the stock tank sediment since this was also output from the plot. The sediment was oven-dried then weighted to determine the total mass of the eroded sediment. The sediment was then sub-sampled by riffling, and was then analysed for particle size distribution.

Upon return to the laboratory, the auto-sampler bottles were weighed, dried then weighed again to determine the suspended sediment concentration. Sediment from the bottle was collected and subsequently analysed for particle size distribution. While it is recognised that particles may be eroded as aggregates, previous studies in similar sandy desert environments (for example Young, 1980; Parsons *et al.*, 1991) have found that particles tend to erode mostly as primary particles. Also, due to the laboratory protocol of drying out collected samples, aggregates may form during the drying process, therefore in order to ensure comparability between samples, the primary particle-size distribution of the eroded sediment was determined, rather than the effective particle size distribution. Particle-size distribution is classified as pebbles (greater than 2 mm), sand (0.0625 - 2 mm), silt (0.003906 – 0.0625 mm) and clay (≤0.003906 mm).

Results

Soil Moisture

The volumetric soil-moisture content over the grass-shrub ecotone exhibited great temporal variation throughout the summers of 2005 and 2006 in response to rainfall received at each plot (Figure 5). For the most part, soil-moisture content is higher in bare-surface soil than soil under vegetation, and the mean soil-moisture content is higher under grass than shrub throughout the range of soil-moisture conditions measured. Thus, the presence of vegetation and its effect on modifying soil properties induces an influence on soil moisture, from the wetting up of the soil, right through the course of the drying out of the soil. The difference in soil-moisture between vegetated soil and unvegetated soil is generally significant ($p \leq 0.05$).

A total of 250 experimental variograms were calculated, and models fitted, to determine the temporal variations in the spatial structure of soil-moisture content at sites over the grass-shrub ecotone. The geostatistical properties of soil moisture distribution are summarised in Figure 6.

On the grass plot there are considerable changes in the range at which soil moisture content shows spatial dependence. Nugget variance is experienced when soils are particularly dry or wet. Thus, under such conditions no spatial dependence is observable at the scale at which soil moisture was monitored. Dry soil-moisture conditions are not always characterised by nugget variance; under dry conditions the range of spatial dependence often exceeded 1 m, which is greater than the range at which vegetation shows spatial dependence (0.7 m). Under very wet conditions, on occasions nugget variance was observed, but the initial wetting-up of the soil during rainfall events was characterised by very high ranges of spatial dependence. For instance, after rainfall on 21st August 2005, the soil-moisture content was high, averaging 21.7 % for bare areas and 20.9 % for grass-covered areas. These high soil-moisture contents were spatially autocorrelated at a range of 3.5 m. At other times when high soil-moisture contents were monitored, the range of autocorrelation was also high, for instance on 08/09/2005, one day after a large runoff event, the soil-moisture content was 19.5 % for bare areas and 17.3 % for grass-covered areas. The corresponding range of spatial dependence for soil moisture was 2.5 m.

On the grass-shrub plot, when spatial dependence was observed in soil-moisture distribution, the strength of spatial dependence was on the whole greater than that observed over the grass plot. High ranges of autocorrelation were observed under both dry and wet soil-moisture conditions. For instance, on 03/08/2005 and 05/08/2005 the soil-moisture content was very low (2.1 %, 1.0 % and 0.7 % for bare, grass and shrub covered surfaces respectively on 03/08/2005 and 2.7 %, 1.4 % and 1.1 % for bare, grass and shrub covered surfaces respectively on 05/08/2005) and the differences in the soil-moisture content between bare and vegetated areas were significant. Under these low soil-moisture conditions, the range of autocorrelation was over 2 m. However, low ranges of spatial dependence were also observed for similarly low soil-moisture conditions, such as those monitored prior to 03/08/2005. At high soil-moisture conditions, the range of spatial autocorrelation was not consistent. For example, immediately after the runoff event on 21/08/2005, no spatial autocorrelation was observable (i.e. nugget variance). On 22/08/2005, the range of spatial autocorrelation was high, at 2.2 m, but this was then proceeded by nugget variance as the soil dried out. During the particularly wet period between 28/07/2006 and 04/08/2007 the high soil-moisture contents were not spatially autocorrelated, but after that they were, at a range of 1 m on 05/08/2007 and 1.1 m on 07/08/2007. At high soil-moisture conditions after the event on 07/09/2006, the soil moisture contents were autocorrelated at a range of 2 m.

The range of spatial dependence on the shrub-grass plot was often similar to that of vegetation (Table 1). During periods of elevated soil moisture content after rainfall events, higher ranges of spatial dependence were experienced, sometimes followed by nugget variance. For example, during the particularly wet period between 28/07/2006 and 07/08/2006, soil-moisture content was autocorrelated at ranges of between 3 and 5 m which is much greater than the range at which vegetation is spatially autocorrelated (Table 1), although on 29/07/2007 the soil-moisture content was not spatially autocorrelated. At lower soil-moisture contents, the range of autocorrelation is comparable to the range at which the vegetation is autocorrelated (1 m) and the strength of the autocorrelation is typically moderate (0.4). Under low soil-moisture conditions nugget variance was observed, indicating that the soil-moisture content was not spatially autocorrelated. For example, on 06/08/2005 the average soil-moisture contents for bare, grass and shrub-covered surfaces were 2.8 %, 1.6

% and 1.3 % respectively and no spatial autocorrelation was observed. However, on other occasions, the low soil-moisture contents were spatially autocorrelated. For example, on 02/08/2005 the average soil-moisture contents for bare, grass and shrub-covered surfaces were 2.5 %, 1.1 % and 1.0 % respectively, which were moderately spatially dependent at a range of 1.3 m.

The ranges at which soil-moisture was spatially autocorrelated on the shrub plot were generally less than those encountered over the grass, grass-shrub and shrub-grass plots. The maximum range was 2.7 m, on 21/08/2005. For the most part however, ranges varied between 0.8 and 1.2 m, thus equal to, or slightly greater than the range at which vegetation was spatially autocorrelated. When no significant difference was found in the moisture content of soil beneath shrubs and soil in bare surface areas, nugget variance was often found, for instance on 23/08/2005 and 24/08/2005.

Runoff

The runoff responses monitored over all plots were characterised by a very rapid runoff response, with very steep rising and recessional limbs, especially over the shrub-grass and shrub plots. The key characteristics of monitored runoff events are presented in Table 2. The largest runoff event was monitored over the shrub-grass plot on 07/09/2006, during which 90 % (6550 l) of rainfall left the plot as surface runoff. The second largest runoff event monitored was over the shrub plot, on 29/08/2006 which generated 6366 l of runoff and had a runoff coefficient of 0.57. Because of the variations in storm characteristics, such as event timing, duration and total rainfall between each plot, direct comparisons of the runoff response of the four plots to the same rainfall event cannot be made. Instead, the rainfall events monitored over each plot are treated as independent events, and the general trends in runoff response in relation to controlling factors over each plot are examined.

The three characteristics of runoff that are examined here are the runoff coefficient (*RC*), the maximum discharge (Q_m) and the total volume of plot runoff (Q_t). The rainfall characteristics considered that may exert a control over runoff dynamics are the total amount of event rainfall (*ER*), the maximum rainfall intensity (*I*) and the 5-minute maximum rainfall intensity (I_5). *ER* was defined as rainfall that occurred 1 hour prior to the onset of runoff and rain that fell until the cessation of runoff.

Runoff Coefficients

The relationships between rainfall characteristics and runoff coefficients were analysed using linear regression. For a given amount of event rainfall, runoff coefficients tend to be greater over shrubland than grassland (Figure 7). Generally, it is observed that with increasing shrub cover, the intercept of the relationship between event rain and runoff coefficient increases, indicating therefore, that runoff commences at a lower threshold of storm size with increasing shrub cover. These observations are in accordance with those of Schlesinger *et al.* (2000) who found that discharge commenced at a lower threshold of storm size in shrublands and low-cover grassland plots. From the grass, grass-shrub, shrub-grass to shrub plot, the slope of the relationship between *ER* and *RC* increases, which indicates that with increasing shrub cover, there is an increase in the strength of the hydrological response to increased rainfall. The relationships between *RC* and *I* and *RC* and I_5 are significant at $p<0.01$ for all but the grass-shrub plot. Over the grass and shrub plot, *RC* is most highly related to *I* (grass: r^2 = 0.77, $p < 0.005$; shrub: $r^2 = 0.75$, $p < 0.005$), while over the grass-shrub and shrub-grass plots *RC* is most highly related to I_5 (grass-shrub: $r^2 = 0.59$, $p = 0.044$; shrub-grass: $r^2 = 0.85$, $p < 0.005$). Regression analysis was carried out to determine the relationship between the percentage vegetation cover over each plot and *RC,* and the relationship between the antecedent soil-moisture content and *RC*. A negative correlation was found between percentage vegetation cover and *RC* ($r^2 = 0.161$, $p = 0.01$). Although antecedent soil-moisture content is a critical factor affecting runoff generation at fine temporal and spatial scales (Cammeraat, 2002), in terms of the overall event-based runoff response from the plot, no clear relationship is apparent, due to the overriding influences of rainfall characteristics such as *ER* and rainfall intensity.

Maximum discharge (Q_m)

There are positive, yet variable relationships between rainfall characteristics and Q_m (Figure 8). The slope of the relationship between Q_m and rainfall characteristics over the shrub plot was steeper than those of the grass and grass-shrub plots, but not as steep as the shrub-grass plot. On the whole, it appears that Q_m was most highly correlated to *I* and I_5, in particular over the grass, grass-shrub and shrub plots.

Total Discharge (Q_t)

The relationships between Q_t and *ER, I* and I_5 all exhibit strong, positive correlations (Figure 9). The slope of the relationships displays an overall increase from the grass through to the shrub plot, although the slope of the relationships over the shrub-grass plots is greater than that of the shrub plot, indicating that for a given amount of *ER, I* or I_5, a greater total runoff response is experienced over the shrub-grass plot. Over the grass-shrub, shrub-grass and the shrub plot, *ER* is most strongly related to Q_t (grass-shrub: r^2 = 0.84, p = 0.040; shrub-grass: r^2 = 0.87, $p \leq 0.0005$; shrub: r^2 = 0.95, $p \leq 0.0005$), while for the grass plot, I_5 is most strongly related to Q_t (r^2 = 0.98, $p \leq 0.0005$). Thus, it is inferred that over the grass plot, I_5 exerts the major control over the total runoff response, while over plots the grass-shrub, shrub grass and shrub plots, *ER* exerts the major control over the runoff response.

Regressions between event rainfall (*ER*) and total runoff (Q_t) for each plot (Figure 10) have been used to model the total amount of runoff for a given amount of rainfall at each plot. Up until an event rainfall of 11 mm, less runoff is generated over the shrub-grass plot compared to the shrub plot. However, at 12 mm of rainfall, more runoff is generated over the shrub-grass plot. Thus, at an amount of event rainfall greater than 11 mm, the runoff response of the shrub-grass plot exceeds that of the shrub plot.

Erosion: Event Sediment Yield

The sediment yield for a single event was estimated as the total amount of sediment trapped in the stock tank. On occasions where it was not possible to empty the stock tanks between events, the sediment yields from the events were mixed and are therefore not included in the event-based analysis. The relationship between the event sediment yield and the main hydrological characteristics of the runoff events (*R*, *I*, I_5, Q_m and Q_t) are investigated. Scatter plots of sediment yield against *R*, *I*, I_5, Q_m and Q_t are presented in Figure 11.

The total amount of erosion from each plot during runoff events increases from plots the grass through to shrub plot. All plots exhibit positive relationships between *ER*, *I*, I_5, Q_m, Q_t and sediment yield. Over the grass-shrub plot, sediment yield was not significantly related to rainfall (*ER, I* and I_5). Over the shrub-grass plot, significant relationships were found between sediment yield and hydrological characteristics (Q_m and Q_t). Over the shrub plot, while significant relationships were found between sediment yield and hydrological characteristics, the strongest correlation was found between sediment yield and I_5. Thus, the two variables with which sediment yield is best correlated are I_5 (with the exception of the shrub-grass plot) and Q_t (with the exception of the grass-shrub plot).

Over the shrub plot4, increases in sediment yield are much greater with increases in R, I, I_5, Q_m and Q_t than over the grass plot, which indicates that event-based erosion is much more responsive to hydrological variables over shrubland compared to grassland. The dynamics of sediment yield over the transition plots are not as clear-cut as for the grass plot and the shrub plot. Over the grass-shrub plot, for lower event rainfall, the resultant sediment yields are similar to those monitored on the grass plot. However, for the largest amount of event rainfall monitored over the grass-shrub plot (26 mm), the corresponding increase in sediment yield is great, more akin to sediment yields monitored over the shrub-grass plot for a similar amount of event rainfall. Similarly, over the grass-shrub plot increases in sediment yield with great increases in I and I_5 (monitored for the same event) are great. Thus, it appears that there is a threshold of rainfall, above which sediment yield becomes greatly increased over the grass-shrub plot, which is likely to be due to an increase in the connectivity of runoff generating areas that enable the sediment detached by rainfall to be transported to the plot outlet. Over the shrub-grass plot, observed increases in sediment yield with increasing rainfall amount and intensity were not as great as those observed over the shrub plot, although increases were much greater than those observed over the grass plot.

While the sediment yield over the shrub plot increased in response to increasing Q_m and Q_t much more than over the grass plot, dynamics operating over the transition plots were more complex. For the largest event monitored over the grass-shrub plot, increases in Q_m and Q_t resulted in sediment yields similar to those monitored over the shrub plot. Over the shrub-grass plot however, increases in sediment yield with increasing Q_m and Q_t were more of the order of sediment yields monitored over the grass plot.

Particle-Size Characteristics of Eroded Sediment by Event

The particle size distributions of eroded sediment monitored during single runoff events over each plot are shown in Figure 12. There is variation in the particle-size distribution of eroded sediment between events on each plot and between plots. For plots 1 and 2, sand accounts for the bulk of sediment eroded for most events. For the higher magnitude runoff events over the grass plot (07/09/2005, 29/08/2006 and 07/09/2006), the proportion of eroded sediment that is sand is less, and the proportion of eroded sediment that is silt is greater. The decrease in the proportion of sand and increase in the proportion of silt eroded during higher-magnitude runoff events applies to the grass-shrub plot, but to a lesser extent. The percentage of eroded sediment on all plots that is within the clay size-fraction is low, generally less than 10 %. For the shrub-grass and shrub plots, the proportion of eroded sediment that is sand is generally less than the grass and grass-shrub plots, while the proportion that is silt is generally greater. Because of the differences in sediment yield over the four plots, in particular, the much greater sediment yields on the shrub plot, some of the slight differences in the particle-size distribution (PSD), such as the proportion of pebbles in eroded sediment from the grass plot being similar to some of the events monitored on the shrub-grass and shrub plots becomes negligible when the total mass of sediment in that size class is considered. For the events shown in Figure 13 for the shrub-grass and shrub plots, for the most-part, a greater proportion of pebbles made up the eroded sediment over the shrub-grass plot compared to the shrub plot.

The events when the proportion of silt eroded exceeds sand over the shrub-grass and shrub plots are the largest erosion events that took place. For the event on 29/08/2006 on the grass plot, which was the second largest runoff event and the second largest erosion event, the amount of silt eroded exceeded the amount of sand eroded which is akin to the dynamics observed over the two largest events over the shrub-grass and shrub plots. On the whole, however, sand dominated the sediment eroded over all plots, followed by silt, clay and then pebbles. The median particle size (D_{50}) was determined for the sediment eroded from each plot for each event monitored (Figure 13). Overall, there is a significant general decrease in D_{50} with increased event sediment yield (r^2= 0.425, p = 0.001) which indicates that with increased sediment yield there is an increase in the more coarse sediment that is eroded from the plots. The D_{50} of sediment eroded from the shrub-grass and shrub plots is generally lower than the D_{50} of sediment eroded from the grass and grass-shrub plots. When the relationship between event sediment yield and D_{50} are considered independently for each plot, the grass plot shows a decrease in D_{50} with increased sediment yield (r^2 = 0.454, p = 0.046), the grass-shrub plot shows a decrease in D_{50} with high sediment yield (r^2= 0.663, p = 0.094), although to a lesser extent than the grass plot. For the shrub-grass plot there is no clear relationship between D_{50} and sediment yield (r^2 = 0.401, p = 0.252). The grass-shrub plot shows a decrease in D_{50} with increased sediment yield (r^2 = 0.606, p = 0.121), similar to that for the grass-shrub plot although the overall, D_{50} of sediment eroded from the shrub plot is coarser than that eroded from the grass-shrub plot.

Enrichment Ratios of Eroded Sediment by Event

The PSD of the matrix soil at each plot may have an affect on the PSD of eroded sediment. A comparison of the particle-size composition of transported sediment with that of the parent soil provides a measure of the particle-size selectivity involved in sediment mobilisation (Martinez-Mena *et al.*, 2000; Stone and Walling, 1997). To investigate how the PSD of the eroded sediment differs from the PSD of the matrix soil, enrichment ratios are determined. The enrichment ratio of sediment in a given particle size class is determined by:

$$E = \frac{P_r}{P_s} \qquad (1)$$

where, E is the enrichment ratio, P_r is the percentage of particles in a given size class in runoff and P_s is the percentage of particles in a given size class in the soil matrix. Ratios >1 show enrichment, whereby sediment in a given size class forms a greater proportion of the eroded sediment relative to the matrix soil (i.e. preferential erosion of this size class). Ratios <1 represent depletion of sediment from a given size class. The overall particle-size distribution of the matrix soil was determined by calculating the average PSD for bare, grass and shrub covered soil and then calculating an overall weighted average PSD according to the percent cover of bare, grass and shrub-covered surfaces. Enrichment ratios of sediment eroded from each plot for discretely monitored events are shown in Figure 14.

Over all four plots, the sediment eroded is much finer than the matrix soil showing the selective erosion of fine sediment. Thus, even though clay comprises a small proportion of the sediment eroded during runoff events, the eroded sediment is still enriched in clay compared to the matrix soil. Pebbles are consistently depleted in eroded sediment compared to the composition of the matrix soil over all plots for all events monitored. The proportion of sand in eroded sediment is fairly similar to that of the matrix soil, although there is some variability between events. The grass, grass-shrub and shrub plots experienced both enrichment and depletion of sand relative to the soil matrix, whilst the sand fraction was always enriched in sediment eroded from the shrub-grass plot, although for all but one event (grass plot, 04/08/2006) the silt fraction of the eroded sediment was enriched, as was clay. Furthermore, for all but one event (shrub plot, 07/09/2005) the degree of clay enrichment was consistently much greater than silt enrichment across all plots.

Within-Event Sediment Dynamics

Understanding the within-event sediment dynamics can aid in interpreting changing processes that operate throughout runoff events. Within-event sediment dynamics are analysed using measurements of sediment that were sampled in suspension using the ISCO 6700 auto-sampler. These measurements do not necessarily represent the true suspended fraction of sediment, since the flow through the super-critical flume is likely to have mixed coarser fractions of sediment, which may thus have been sampled by the auto-sampler. Therefore, although the sediment sampled in suspension by the auto-sampler is neither representative of the true suspended sediment fraction, or total amount of sediment in the runoff, the analysis of the amount and particle-size distribution of sediment at the point of sampling can still provide a valuable insight into erosion dynamics throughout the runoff events. In order to obtain a greater understanding of the dynamics of erosion over each plot, and the relative losses of coarse and fine sediments, particle size analysis was undertaken (where there was enough sediment sampled for analysis, typically > 1 g). The particle size of eroded sediment may provide basic information about erosion processes over each plot. Examples of the sediment flux throughout runoff events and the particle-size distribution of eroded sediment are shown in Figure 15.

The amount of sediment monitored in runoff, and the particle-size distribution of the eroded sediment was variable between events and between plots. The particle-size characteristics of sediment over all plots generally show a decline in the proportion of sand and an increase in the proportion of silt, and in particular, clay throughout the events. Over the grass plot, on 29/08/2006, the initial peak in Q at the start of the runoff event had a sediment flux of 42 g min^{-1} at 33.6 l min^{-1}, which was comprised of 41 % sand, 44 % silt and 15 % clay. Hysteretic properties are evident, as sediment flux declined to 11 g min^{-1} before peak Q is reached, which was comprised of 16 % sand, 59 % silt and 25 % clay. At the main peak of the storm hydrograph, about 17 minutes after the first runoff peak, suspended sediment again displayed hysteretic properties. At the peak sediment flux (355 g min^{-1}, with Q of 218 l min^{-1}) at 04:02 am, the particle-size characteristics were 53 % sand, 42 % silt and 5 % clay. The composition of the last suspended sediment sample at 04:18 when Q was 31 l min^{-1} and suspended sediment flux, was 4 g min^{-1}, was 12 % sand, 63 % silt and 25 % clay. Thus, the composition of suspended sediment at the end of the recessional limb of the first runoff peak and the second runoff peak at comparable discharges was very similar. For the event on 07/09/2006, on the rising limb of the sedigraph, the proportion of sand that made up the suspended sediment increased until the peak suspended sediment flux of 108 g min^{-1}, when the discharge was 66 l min^{-1}, and the sediment was comprised of 62 % sand, 32 % silt and 6 % clay. The proportion of sand that made up the suspended sediment declined thereafter. At a lower point on the recessional limb at 01:27 am when the discharge was 34 l min $^{-1}$ and the suspended sediment flux was 18 g min^{-1}, the make-up of the suspended sediment was 3 % sand, 51 % silt and 46 % clay. The discharge of 34 l min^{-1}, comparable to the discharge at 04:18 am on 29/08/2006 yielded a greater suspended sediment flux and a different particle-size distribution.

For the sediment dynamics monitored over the grass-shrub plot on 07/09/2005, 15/08/2006 and 07/09/2006, behaviour of both the rising and recessional limbs was poorly captured, although the data obtained are still adequate to provide an insight into the composition of sediment throughout the events. During the rising limbs of the 07/09/2005 and 07/09/2006 events, there is a gradual increase in the proportion of suspended sediment that is made up of sand. As was similarly observed over the grass plot, for the larger of the two events (07/09/2005), a lower proportion of the suspended sediment was made up of sand, although the actual flux of sand was greater for the 07/09/2005 event, when the peak flux of sand was 88 g min^{-1}, compared to 07/09/2006 when the peak flux of sand was 38 g min^{-1}. During the 15/08/2006 event, which was much smaller, with a peak Q of 48 l min $^{-1}$ and peak suspended sediment flux of 13 g min^{-1}, only three sediment samples were taken.

At the shrub-grass plot, for the events that occurred on 01/07/2006 and 31/07/2006, dynamics similar to those observed over the grass and grass-shrub plots were monitored, in which the proportion of sand decreased throughout the event. The events that occurred on 31/07/2006, 01/08/2006, 11/08/2006 and 29/08/2006 show an increase in the proportion of clay throughout the event. For the largest event monitored (on all of the plots) on 07/09/2006, where Q reached 479 l min^{-1}, changes in the composition of suspended sediment arose primarily when there were increases in Q. It is possible that increases in Q increased the entrainment of coarser sediment thereby increasing the proportion of sand making up the eroded sediment. On the shrub plot there is a consistent decrease in the proportion of sand and increase in the proportion of silt and clay throughout events, as has been observed over the other plots.

Discussion

Soil Moisture

There are clear spatial and temporal variations in soil-moisture content over the grass-shrub ecotone (Figures 5 and 6). It is already well established that water exerts a primary control over net primary productivity in semi-arid ecosystems (Huenneke *et al.* 2002). Thus, the temporal dynamics of changes in soil-moisture content and spatial patterns are important in terms of understanding variations in water available for plants to uptake. The soil-moisture content of the bare-surface soil is generally higher than that under vegetation, except during particularly wet conditions when the difference in soil-moisture content between bare and vegetated soils decreases. The differences in soil characteristics and water uptake by plants between the bare-surface soil and soil under vegetation create a difference in the retention of water in the soil, leading to the observed differences in variation of soil moisture and differences between the different surface cover types (see Turnbull *et al*., *in review*). It is likely that the increased fragmentation of grass on the grass-shrub plot compared to the grass plot creates a wider range of soil-plant feedbacks and thus modifications to the soil and uptake of water usage by plants, resulting in greater variation in soil moisture content under grass. On the shrub plot, on occasions when no significant difference was found in the soil-moisture content beneath shrubs and bare soil, nugget variance was often found, which indicates that it is the vegetational effects on soil-moisture content due to plant uptake of water, and improved soil structure under vegetation that exert a great influence on the spatial autocorrelation of soil-moisture content over shrubland. The most noticeable change in the spatial structure of soil moisture is when the soil becomes very wet, and the range of spatial autocorrelation greatly increases. Since increases in soil-moisture content arise from rainfall events which may generate runoff, it is hypothesised that these increases in the range of autocorrelation are due to the effects of the redistribution of water over the landscape, the range of which will depend upon the structure of the ecosystem and rainfall characteristics.

Distinct changes in the spatial distribution of soil-moisture content over each plot were observed through time, In this study, in the case of soil-moisture content where the temporal changes in spatial distribution were addressed, there were distinct changes in the range of spatial dependence, which are likely to be due to the temporal changes in local versus non-local controls on soil-moisture distribution (Grayson *et al.*, 2006). Non-local controls occur under wet conditions and are determined by lateral water movement (i.e. runoff), while local controls predominate under non-runoff, drier conditions when vertical water fluxes dominate. The interpretation of changing controls over soil-moisture dynamics of Grayson *et al*. (1998; 2006) in semi-arid areas is in accordance with the temporal changes in spatial patterns of soil-moisture distribution found here. After the occurrence of runoff during rainfall events, larger ranges of spatial dependence were observed. Upon drying out of the soil, soil-moisture content was higher in the unvegetated surface soil than the vegetated surface soil, which is likely to be due to increased transpiration of soil moisture under vegetation. Furthermore, under shrubs, the channelisation by stemflow of rainfall intercepted by the shrub to deep tap-roots reduces the amount of water that is available to be stored in the surface soils (Martinez-Meza and Whitford, 1996; Whitford *et al.*, 1997; although these authors over-emphasize the effect: Abrahams *et al.*, 2003). Thus, over the grass-shrub ecotone, non-local controls with a larger range of spatial dependence dominate soil-moisture dynamics under wet conditions, while local controls have an increased influence on soil-moisture dynamics under drier conditions. Over shrubland, the greater strength of spatial dependence due to the shrub-occupied islands of fertility, created by plant-soil feedbacks, reinforces the role of local controls on soil-moisture distribution, explaining why fewer occasions were monitored over shrubland when the range of spatial dependence of soil-moisture distribution was larger than the range of spatial dependence of the shrubs. Variability was observed in the ranges at which soil moisture is autocorrelated for a given soil-moisture content. This indicates that differences in processes (for example runoff, plant uptake of water, evaporation and transpiration) operating through time and over multiple spatial scales give rise to differences in the resultant patterns of soil-moisture content over the landscape. For instance, for high plot-average soil-moisture content, the range of spatial autocorrelation may be high on some occasions, and non-existent on others. The spatially and temporally variable distribution of soil-moisture at stages over the transition from grassland to shrubland exerts a great control over other ecosystem processes, in particular, runoff generation, plant-water availability and nutrient cycling.

Runoff

Results from the grass-shrub, shrub-grass and shrub plots suggest that *ER* exerts the primary control over Q_t, while over the grass plot, I_5 appears to exert the primary control over Q_t. The differences in the apparent controlling factors of runoff are likely to be related to the surface characteristics of each plot. As the cover decreases and becomes increasingly fragmented over the grass-shrub ecotone, the increasingly well-connected flow pathways increase the propensity for runoff-generating areas to become connected due to decreased transmission losses (Parsons *et al.*, 1996), and therefore yield a runoff response that is well synchronised with event rainfall. Over the grass plot however, the high grass cover, and large grass patches means that runoff-generating areas are relatively disconnected. Therefore, over the grass plot, because of the disconnectivity of runoff-generating areas, the runoff response at the plot outlet is not so well synchronised with event rainfall. Hence, over the grass plot, Q_t is better related to I_5 than I, since sustained periods of high-intensity rainfall facilitate prolonged runoff generation enabling runoff generating areas to become connected, thus yielding a hydrological response at the plot outlet. The relationship between Q_m and rainfall characteristics was very similar for the grass and grass-shrub plots, although the slope of the relationships for the grass-shrub plot are slightly greater than that for the grass plot, indicating that surface characteristics over the grass-shrub plot, such as increased connectivity of bare areas relative to the grass plot, enable a more rapid runoff response to short bursts of intense rainfall, with runoff attaining greater discharges more quickly. The events monitored over grassland show that they do in fact generate high amounts of runoff and yield relatively high runoff coefficients under high magnitude rain events with high rainfall intensities. For example, the event on 29/08/2006 over the grass plot had a runoff coefficient of 0.41, which is comparable to runoff coefficients monitored over the shrub-grass and shrub plots. Although grasslands do not tend to experience runoff coefficients as high as those experienced where there is a greater shrub cover, grasslands do have the potential to yield high runoff coefficients, which suggests that previous conceptions of grasslands as being 'non-leaky' (e.g. Bastin *et al.*, 2002; Ludwig *et al.*, 2002) may need to be rethought under certain conditions. It is likely that the connectivity of the runoff-generating areas in high magnitude rainfall events increases with increases in flow depth, as the stepped microtopography (which inhibits connected flow in smaller runoff events) is exceeded. Thus, in grasslands there may be a threshold amount of rainfall, above which runoff coefficients in grasslands and shrublands are comparable.

While it was not possible to replicate experiments at each stage over the transition from grassland to shrubland, results clearly suggest that the increase in runoff over the grassland to shrubland transition does not appear to follow a linear trajectory, since under certain conditions, primarily the largest rainfall events monitored, the shrub-grass plot was found to generate greater runoff coefficients than the shrub plot. Since the plots at stages over the transition are different in terms of their vegetation cover, distribution and soil-surface characteristics (see Turnbull *et al.* in review), it is apparent that the change in structural connectivity of biotic and abiotic components of the ecosystem in combination with rainfall characteristics, governs the functional connectivity of the hydrological response. These findings are in accordance with those of Müller *et al.* (2007), who found that, in order to model accurately the correct hydrological response over semi-arid grassland and shrubland, the proper representation of the spatial connectivity of hydrologic parameters is critical, which thus highlights the sensitivity of the hydrologic response to the spatial structure of the ecosystem.

Erosion

There are several factors that determine the amount of erosion from semi-arid hillslopes, primarily related to issues of sediment supply and transport. For example, the amount of sediment that is detached by rainfall, the extent to which surface crusts or stone pavements are developed that form a protective layer and reduce sediment detachment rates and ultimately, the competency of the overland flow to transport the detached sediment that determines the overall erosion rates (Parsons *et al.*, 1994; Wainwright *et al.*, 2000). Processes such as sediment detachment by raindrop impact are affected by the structural components of the ecosystem (see Turnbull *et al.* in review). For instance, raindrop impact breaks and disperses aggregates at the soil surface, which releases sediment at the soil-surface that can be transported by overland flow (Lado and Ben-Hur, 2004). Thus, the differences in vegetation and soil-structure characteristics, such as soil-particle size characteristics, pavement cover and soil-aggregate stability can affect the functional response of the ecosystem in terms of the erosion and sediment redistribution, which modify further the structure of the ecosystem. The observed differences in the erosion response between the plots indicate that the different surface characteristics affect the total amount of sediment that is eroded due to surface flow characteristics, the supply of readily entrainable sediment, surface cover, and the area of the plot that is contributing runoff and entrained sediment to the base of the plot. For instance, the presence of vegetation – even sparse creosotebush canopies – has the effect of reducing the kinetic energy of rainfall (Wainwright *et al.*, 1999), which will reduce sediment detachment by rainfall.

Over the grassland to shrubland transition, the connectivity of bare areas, where runoff tends to be preferentially generated, increases. Therefore, from the grass, grass-shrub, shrub-grass to shrub plots, flow lines become increasingly well connected which increases the capacity for flow to entrain and transport sediment, leading to the greater sediment yields monitored over shrubland. For example, the greater runoff response of the shrub-grass and shrub plots that enables higher discharges to be reached will increase the potential for erosion to take place because of the greater amount of energy available to detach and entrain sediment. However, factors such as sediment supply do come into play. The largest runoff event monitored was on the shrub-grass plot. However, in spite of the relatively well-connected flow lines and high amount of runoff that reached the plot outlet (6550 l with a RC of 0.9), the sediment yield was only 6178 g (i.e. 0.93 g/l). The event with the largest sediment yield was monitored over the shrub plot, which generated 2174 l of runoff, with a RC of 0.51 and had a sediment yield of 10823 g (i.e. 4.98 g/l). The armouring of the stone pavement over the shrub-grass plot is likely to have reduced the detachment of sediment by raindrop action (Wainwright *et al.*, 1995) (hence the low correlation between sediment yield and rainfall characteristics over the shrub-grass plot), thus affecting the supply of readily entrainable sediment.

On the grass and grass-shrub plots, it is likely that the majority of runoff and sediment eroded from the plot was sourced from the lower part of the plot, particularly during smaller runoff events, because of the pitted microtopography and other surface characteristics, which reduce the connectivity of runoff-generating areas. Therefore, when runoff is generated on the grass plot, the configuration of runoff generating areas and flow lines has the effect of reducing the capacity of the flow to transport the entrained sediment over longer distances. Consequently, sediment yields over the grass plot remained low compared to the other plots. On the grass-shrub plot, when lower volumes of runoff were generated, sediment yields were akin to those measured over the grass plot. However, results show that at greater volumes of runoff, there is an increase in erosion from the grass-shrub plot (for example the events on 07/09/2005, 15/08/2006 and 07/09/2006). The largest event (07/09/2005) shows that the composition of suspended sediment is more comparable to the 15/08/2006 sediment. It is plausible that differences in flow connectivity between all three events account for the differences in both amount and composition of suspended sediment. For instance, during the smaller event on 15/08/2006, it is likely that runoff-generating areas were not well connected. Therefore, the runoff would not have attained such high velocities compared to larger events and the flow would have had a reduced capacity to entrain and transport coarser sediment such as sand, thus possibly explaining the low proportion of sand that makes up the eroded sediment in this event. During the 07/09/2006 event, the flow has a greater capacity to entrain sediment, but limited flow connectivity over the plot means that the bulk of the sediment reaching the plot outlet is sediment that is entrained from the lower part of the plot. Here, the supply of entrainable fines becomes exhausted, hence the greater proportion of sand making up the suspended sediment. For the largest event on 07/09/2005, it is likely that a threshold of connectivity was exceeded, resulting in the transport of silt and clay from upslope areas, thus increasing the proportion of silt and clay making up the plot sediment yield. Thus, it is likely that the increase in bare surface area on the grass-shrub plot increases the connectivity of runoff generating areas once a threshold of functional connectivity is surpassed, thus enabling sediment entrained from further upslope to be transported over longer distances.

One explanation for the lower sediment yields on the shrub-grass plot is that the supply of entrainable sediment has already been eroded from the plot. The high percentage of stone-pavement cover over the shrub-grass plot is likely to protect the surface from raindrop impact (Poesen and Lavee, 1994) and therefore reduce the amount of sediment that is detached by rainfall, even though it increases runoff coefficients. Therefore, it appears that erosion occurring on the shrub-grass plot is supply-limited rather than transport limited. Conversely, on the grass-shrub plot, it is reasonable to assume that sediment yields are transport-limited rather than supply limited, since once high discharges are attained, there is a high sediment yield from the plot.

Other studies in semi-arid environments have also found that the cover and configuration of vegetation patches affects the sediment yield from plots. For instance, in semi-arid Australian savannah, Ludwig *et al*. (2007) found that sediment yields from hillslopes were strongly dependent upon fine versus coarse-grained patch structure, and on semi-arid Mediterranean hillslopes, Bautista *et al.* (2007) found that decreasing patch density or coarsening of the spatial pattern of the patch-interpatch system leads to an increase in runoff and sediment yields. Another factor that may cause erosion to be lower when there is high vegetation cover is the effect of vegetation and litter on protecting the soil surface from rainfall impact, thus potentially reducing the detachment of soil particles (Dunjó *et al.*, 2004; Wainwright *et al.*, 1999) and reducing the supply of material to be eroded. The differences in soil moisture content between vegetated and bare areas is likely to have an effect on erosion rates, since over grassland and shrubland the bare soil typically has a higher surface-soil-moisture content, which can lead to a decrease in surface-soil shear strength which can cause detachment rates to increase (Parsons *et al.*, 1994). Thus, the detachment of sediment may be affected by the spatio-temporal evolution of soil-moisture content over the ecosystem.

Decreases in the flux of sediment from the plots throughout the runoff events were observable, and are likely to be due to the development of surface crusts, caused by the compression of the soil surface or the deposition of fine particles in pore spaces (Romkens *et al.*, 1990). On crust-covered surfaces, the crust may reduce erosion rates, since once all loose sediment has been eroded the crust may form a protective surface that is difficult to erode, due to the increased cohesion of soil particles and increased soil surface strength (Luk and Cai, 1990). The particle-size characteristics of eroded sediment may help to constrain the controls on erosion in operation throughout runoff events. Over all of the plots, the eroded sediment is finer than the matrix soil, which is in accordance with previous field and laboratory-based observations (e.g. Malam Issa *et al.*, 2006; Parsons *et al.*, 1991), who attributed this to the selective detachment of sediment by raindrops and selective transport by interrill overland flow. Furthermore, the preferential deposition of coarser sediment during flow will further re-enforce the particle-size selectivity of eroded sediment. Results are indicative that as sediment yield increases, the size-selectivity of sediment that is eroded from the plots changes, and ultimately becomes more fine in relative terms, although in absolute terms, the amount of coarse sediment eroded increases probably due to the increased hydrological energy available for sediment entrainment and transport. The change in particle-size distribution of the eroded sediment is suggestive that for the larger events on the grass, grass-shrub and shrub plots, fine sediment eroded from upslope areas is able to reach the base of the plot, which results in the apparent enrichment of the fine sediment fraction compared to smaller events. The sediment eroded from the shrub-grass and shrub plots is generally more enriched with fine sediment than the sediment that is eroded from the grass and grass-shrub plots in relative terms, which is likely to be due to the increased connectivity of flow over these plots, that enables the fine sediment eroded from upslope areas to be transported to the base of the plot due to the selective transport of fine sediment by runoff, whilst in the upslope areas it is likely that the flow has a transport capacity that is too low to transport more coarse material to downslope areas. It is also possible that if coarse sediment is transported by flow, it can quickly become trapped in depressions, leaving a lag deposition of fine sand and fine gravel (Gabet and Dunne, 2003) which is unlikely to become re-detached in areas of low flow velocity (such as in upslope areas), thus resulting in the selective transport of fines down the slope to the plot outlet.

The selective erosion of fine sediment may contribute over time, to the development of stone pavements, which are predominant in degraded landscapes. In areas where the stone-pavement cover is particularly well-developed, such as on the shrub-grass plot, much of the available sediment supply has already been exhausted, hence why the largest runoff event measured (on the shrub-grass plot) did not have the largest sediment yield measured.

The findings of this study are likely to be scale-dependent. Previous research (Brazier *et al.*, 2006; Parsons *et al.*, 2006) has demonstrated the effects of scale on hydrology, erosion and dissolved nitrogen losses in runoff. For instance, although results indicate that high runoff and erosion are possible from grassland, it might be the case that under high-magnitude rainfall events there is an increase in the scale of redistribution of water, sediment and nutrients, rather than a net loss from the ecosystem. Obviously, other broader-scale factors, such as the geomorphological setting (for example, the proximity to well-connected flow lines such as ephemeral channels and the position on a hillslope) determine the extent to which water, sediment and nutrients are redistributed around the ecosystem or lost to downstream channels. Therefore, the results presented in this study cannot be simply linearly extrapolated to the broader landscape-scale without full consideration of the effects of scale on runoff, erosion and nutrient fluxes. However, by considering the structural and functional connectivity over a continuum of spatial and temporal scales, it will be possible to determine the landscape-scale runoff, erosion and nutrient response.

Conclusions

The results of this study have provided new insight into spatio-temporal soil-moisture dynamics at stages over a transition from semi-arid grassland to shrubland, revealing the importance of local and non-local controls on soil-moisture dynamics. Results have shown significant differences in the hydrological response to rainfall events over the grass-shrub transition. A comparison between the grassland and shrubland end-member plots suggest that much more runoff is generated over shrubland, as would be expected. However, the results from the transition plots suggest that the changes in runoff dynamics over the trajectory of degradation from grassland to shrubland are more complex. The regressions between *ER* and Q_t for each plot (Figure 11) suggest a non-linear change in plot runoff with increased rainfall at points over the transition from grassland to shrubland, with the greatest runoff observed over the shrub-grass plot. The amount and characteristics of erosion increase at stages over the transition from grassland to shrubland. Results suggest that the changes in surface characteristics over the transition from grassland to shrubland (Turnbull *et al.* in review) in combination with changes in hydrological response over the transition from grassland to shrubland determine the capacity of the runoff to detach, entrain and transport sediment. The selective erosion of fine sediment may be particularly significant in terms of nutrient losses and nutrient cycling, since the progressive selective erosion of nutrient-rich fine sediment may lead to the degradation of the soil. Ultimately, changes in soil moisture, runoff and erosion are significant over the transition from grassland to shrubland. The results presented in this paper suggest that these changes are not linear, thus highlighting the importance of looking at the dynamics of change during vegetation transitions, and not only at differences between processes between two end-member vegetation states.

Acknowledgements

We gratefully acknowledge support for this research from the University of Sheffield and NSF award DEB-0217774 to the University of New Mexico for Long-Term Ecological Research at the Sevilleta National Wildlife Refuge. Assistance at Sevilleta was generously provided by Scott Collins, Jennifer Johnson, John de Witt, Jim Elliot and Mike Friggens. The Worshipful Company of Farmers and the Royal Society Dudley Stamp Memorial Fund are also thanked for providing a travel bursary to undertake the fieldwork. In particular, many thanks to Paul Coles for redrawing all the figures in this paper.

References

Abrahams AD, Parsons AJ. 1991. Relation between infiltration and stone cover on a semiarid hillslope, Southern Arizona. *Journal of Hydrology* **122**: 49-59.

Abrahams AD, Parsons AJ, Wainwright J. 1994. Resistance To Overland-Flow On Semiarid Grassland And Shrubland Hillslopes, Walnut Gulch, Southern Arizona. *Journal of Hydrology* **156**: 431-446.

Abrahams, AD, Parsons AJ, Wainwright J. 2003. Disposition of stemflow under creosotebush. *Hydrological Processes* **17**: 2555–2566 .

Bautista S, Mayor AG, Bourakohuadar J, Bellot J. 2007. Plant spatial pattern predicts hillslope runoff and erosion in a semiarid Mediterranean landscape. *Ecosystems* **10**: 987 - 998.

Bastin GN, Ludwig JA, Eager RW, Chewings VH, Liedloff AC. 2002. Indicators of landscape function: comparing patchiness metrics using remotely-sensed data from rangelands. *Ecological Indicators* **1**: 247 - 260.

Bergkamp G. 1998. A hierarchical view of the interactions of runoff and infiltration with vegetation and microtopography in semiarid shrublands. *Catena* **33**: 201-220.

Bhark EW, Small EE. 2003. Association between plant canopies and the spatial patterns of infiltration in shrubland and grassland of the Chihuahuan Desert, New Mexico. *Ecosystems* **6**: 185-196.

Boix-Fayos C, Martínez-Mena M, Calvo-Cases A, Arnau-Rosalén E, Albaladejo J, Castillo V. 2007. Causes and underlying processes of measurement variability in field erosion plots in Mediterranean conditions. *Earth Surface Processes and Landforms* **32**: 85–101.

Brazier RE, Parsons AJ, Wainwright J, Powell MD, Schlesinger WH. 2006. Upscaling understanding of nutrient dynamics associated with overland flow in a semi-arid environment. *Biogeochemistry*. DOI: 10.1007/s10533-007-9070-x

Buffington LC, Herbel CH. 1965. Vegetational changes on a semidesert grassland range from 1858 to 1963. *Ecological Monographs* **35**: 139 - 164.

Buttafuoco G, Castrignano A, Busoni E, Dimase AC. 2005. Studying the spatial structure evolution of soil water content using multivariate geostatistics. *Journal of Hydrology* **311**: 202 - 218.

Cambardella CA, Moorman TB, Novak JM, Parkin TB, Karlen DL, Turco RF, Konopka AE. 1994. Field-scale variability of soil properties in central Iowa soils. *Soil Science Society of America Journal* **58**: 1501 - 1511.

Cammeraat LH (2002) A review of two strongly contrasting geomorphological systems within the context of scale. *Earth Surface Processes and Landforms* **27**: 1201-1222.

Charley JL, West NE. 1975. Plant-Induced Soil Chemical Patterns in Some Shrub-Dominated Semi-Desert Ecosystems of Utah. *Journal of Ecology* **63**: 945 - 963.

Dunjo G, Pardini G, Gispert M. 2004. The role of land use-land cover on runoff generation and sediment yield at a microplot scale, in a small Mediterranean catchment. *Journal of Arid Environments* **57**: 99-116.

Fernandez-Illescas CP, Porporato A, Laio F, Rodiguez-Iturbe I. 2001. The ecohydrological role of soil texture in a water-limited ecosystem. *Water Resources Research* **37**: 2863 - 2872.

Gabet EJ, Dunne T. 2003 Sediment detachment by rain power. *Water Resources Research* **39**: 1 - 11.

Gosz JR. 1992. Ecological Functions in a Biome Transition Zone: Translating Local Responses to Broad-Scale Dynamics. In *Landscape Boundaries: Consequences for Biotic Diversity and Ecological Flows*, Hansen AJ, di Castri F (eds). Springer-Verlag: Berlin; 55 - 75.

Gosz JR. 1993. Ecotone Hierarchies. *Ecological Applications* **3**: 369 - 376

Grayson RB, Western AW. 1998. Towards areal estimation of soil water content from point measurements: time and space stability of mean response. *Journal of Hydrology* **207**: 68 - 82.

Grayson RB, Western AW, Walker JP, Kandel DD, Costelloe JF, Wilson DJ. 2006. Controls on patterns of soil moisture in arid and semi-arid systems. In *Dryland Ecohydrology*, D'Odorico P, Porporato A (eds). Springer: Dordrecht; 109 - 128.

Gustafson EJ. 1998. Quantifying landscape spatial pattern: What is the state of the art? *Ecosystems* **1**: 143 - 156.

Huenneke LF, Anderson J, Muldavin E, Schlesinger WH. 2002. Spatial and temporal variation in aboveground biomass and net primary production in Chihuahuan Desert ecosystems. *Global Change Biology* **8**: 247-264.

Huenneke LF, Schlesinger WH. 2004. Patterns Net Primary Production in Chihuahan Desert Ecosystems. In *Structure and Function of a Chihuahuan Desert Ecosystem: The Jornada Basin Long-Term Ecological Research Site*, Havstad KM, Huenneke LF, Schlesinger WH (eds). Oxford University Press: Oxford; 232 - 246.

Humphrey RR. 1953. The Desert Grassland, Past and Present. *Journal of Range Management* **6**: 159 - 164.

Humphrey RR. 1958. The Desert Grassland: A history of vegetational change and an analysis of causes. *Botanical Review* **24**: 193 - 252.

ISCO (2005) *ISCO Product Data: 730 Bubbler Flow Module* Teledyne ISCO, Lincoln, Nebraska

Krueger T, Quinton J, Freer J, Macleod CJA, Bilotta GS, Brazier RE, Butler P, Granger S, Haygarth PM. (2009) Uncertainties in data and models to describe event dynamics of agricultural sediment and phosphorus transfer. *Journal of Environmental Quality* **38**: 1137 - 1148

Kurc SA, Small EE. 2007. Soil moisture variations and ecosystem-scale fluxes of water and carbon in semiarid grassland and shrubland, *Water Resources Research* 43, art. no. W06416, doi:10.1029/2006WR005011.

Lado A, Ben-Hur A. 2004. Soil mineralogy effects on seal formation, runoff and soil loss. *Applied Clay Science* **24**: 209-224.

Ludwig JA, Eager RW, Bastin GN, Chewings VH, Liedloff AC. 2002. A leakiness index for assessing landscape function using remote sensing. *Landscape Ecology* **17**: 157-171.

Ludwig JA, Bartley R, Hawdon A, Abbott B, McJannet D (2007) Patch configuration nonlinearly affects sediment loss across scales in a grazed catchment in North-east Australia. *Ecosystems* **10**: 839-845

Luk SH, Cai QG. 1990. Laboratory experiments in crust development and rainsplash erosion of loess soils, China. *Catena* **17**: 261 - 267.

Malam-Issa O, Le Bissonnais Y, Planchon O, Favis-Mortlock D, Silvera N, Wainwright J. 2006. Soil detachment and transport on field- and laboratory-scale interill areas: erosion processes and the size-selectivity of eroded sediment. *Earth Surface Processes and Landforms* **31**: 929 - 939.

MartinezMeza E, Whitford WG. 1996. Stemflow, throughfall and channelization of stemflow by roots in three Chihuahuan desert shrubs. *Journal of Arid Environments* **32**: 271-287.

Martinez-Mena M, Rogel JA, Albaladejo J, Castillo VM. 2000. Influence of vegetal cover on sediment particle size distribution in natural rainfall conditions in a semiarid environment. *Catena* **38**: 175-190.

Müller EN, Wainwright J, Parsons AJ. 2007. The stability of vegetation boundaries and the propagation of desertification in the American Southwest: a modelling approach. *Ecological Modelling* **208**: 91 - 101.

Müller EN, Wainwright J, Parsons AJ. 2008. Spatial variability of soil and nutrient parameters within grasslands and shrublands of a semi-arid environment. *Ecohydrology* **1**: 1 - 14.

Neave M, Abrahams AD. 2002. Vegetation influences on water yields from grassland and shrubland ecosystems in the Chihuahuan Desert. *Earth Surface Processes and Landforms* **27**: 1011-1020.

Noy-Meir I. 1973. Desert ecosystems: environment and producers. *Annual Review of Ecology and Systematics* **4**: 25-41.

Parsons AJ, Abrahams AD, Luk S. 1991. Size characteristics of sediment in interill overland flow on a semi-arid hillslope, Southern Arizona. *Earth Surface Processes and Landforms* **16**: 143 - 152.

Parsons AJ, Abrahams AD, Wainwright J. 1994. Rainsplash and erosion rates in an interrill area on semiarid grassland, Southern Arizona. *Catena* **22**: 215-226.

Parsons AJ, Abrahams AD, Wainwright J. 1996. Responses of interrill runoff and erosion rates to vegetation change in southern Arizona. *Geomorphology* **14**: 311-317.

Parsons AJ, Brazier RE, Wainwright J, Powell DM. 2006. Scale relationships in hillslope runoff and erosion. *Earth Surface Processes and Landforms* **31**: 1384-1393.

Poesen J, Lavee H. 1994. Rock fragments in top soils: significance and processes. *Catena* **23**: 1-28.

Romkens MJ, Prasa SN, Whisler FD. 1990. Surface sealing and infiltration. In *Processes in Hillslope Hydrology*, Anderson MG, Burt TP (eds). Wiley: New York; 127 - 172.

Schlesinger WH, Reynolds JF, Cunningham GL, Huenneke LF, Jarrell WM, Virginia RA, Whitford WG. 1990. Biological feedbacks in global desertification. *Science* **247**: 1043 - 1048.

Schlesinger WH, Raike JA, Hartley AE, Cross AF. 1996. On the spatial pattern of soil nutrients in desert ecosystems. *Ecology* **77**: 364 - 374.

Schlesinger WH, Ward TJ, Anderson J. 2000. Nutrient losses in runoff from grassland and shrubland habitats in southern New Mexico: II. Field plots. *Biogeochemistry* **49**: 69 - 86.

Sevilleta LTER 2008 'Sevilleta Long Term Ecological Research', http://sev.lternet.edu/ [Last accessed 11th December 2008]

Stone PM, Walling DE. 1997. Particle size selectivity considerations in suspended sediment budget investigations. *Water Air and Soil Pollution* **99**: 63-70.

Snyder KA, Mitchell KA, Herrick JE. 2005. Patterns and Controls of Soil Water in the Jornada Basin. In *Structure and Function of a Chihuahuan Desert Ecosystem: The Jornada Basin Long-Term Ecological Research Site*, Havstad KM, Huenneke LF, Schlesinger WH (eds). Oxford University Press: Oxford; 107 - 132.

Turnbull L, Wainwright J, Brazier RE. 2008. A conceptual framework for understanding semi-arid land degradation: ecohydrological interactions across multiple space-and time scales. *Ecohydrology* **1**: 23 - 34. DOI: 10.1002/eco.4

Turnbull L, Wainwright J, Brazier RE. in review. Changes in ecosystem structure over a semi-arid grassland to shrubland transition. *Ecosystems*.

Turnbull L, Wainwright J, Brazier RE. in review. Modelling hydrology, erosion and nutrient transfers over a semi-arid transition from grassland to shrubland in the South-Western USA

Wainwright, J 2009. Desert ecogeomorphology. In *Geomorphology of Desert Environments*, 2nd ed, Parsons AJ and Abrahams AD (eds). Springer, Berlin.

Wainwright J, Parsons AJ, Abrahams AD. 1995. A simulation study of the role of raindrop erosion in the formation of desert pavements. *Earth Surface Processes and Landforms* **20**: 277- 291.

Wainwright J, Parsons AJ, Abrahams AD. 1999. Rainfall energy under creosotebush. *Journal of Arid Environments* **43**: 111-120.

Wainwright J, Parsons AJ, Abrahams AD. 2000. Plot-scale studies of vegetation, overland flow and erosion interactions: case studies from Arizona and New Mexico. *Hydrological Processes* **14**: 2921-2943.

Wainwright J, Parsons AJ, Schlesinger WH, Abrahams AD. 2002. Hydrology-vegetation interactions in areas of discontinuous flow on a semi-arid bajada, Southern New Mexico. *Journal of Arid Environments* **51**: 319 - 338.

Wainwright J, Parsons AJ, Muller EN, Brazier RE, Powell M, Fenti B. 2008a. A transport distance approach to scaling erosion rates: 3. Evaluating scaling characteristics of MAHLERAN. *Earth Surface Processes and Landforms*. DOI: 10.1002/esp.1622

Wainwright J, Parsons AJ, Muller EN, Brazier RE, Powell M, Fenti B. 2008b. A transport distance approach to scaling erosion rates: 2. Sensitivity and evaluation of MAHLERAN. *Earth Surface Processes and Landforms*. DOI: 10.1002/esp.1623

Whitford WG, Anderson J, Rice PM. 1997. Stemflow contribution to the 'fertile island' effect in creosotebush, Larrea tridentata. *Journal of Arid Environments* **35**: 451-457.

Young RA. 1980. Characteristics of eroded sediment. *Transactions of the American Society of Agricultural Engineers* **23**: 1139-1142.

List of Tables

List of Figures

Figure 1. Location of the Sevilleta National Wildlife Refuge (SNWR) in the south-western USA and the location of the four study sites within the SNWR (grass = plot 1, grass-shrub = plot 2, shrub-grass = plot 3 and shrub = plot 4).

Figure 2. Selected study sites over the grass-shrub transition, from the grass end-member (plot 1) across the grass-shrub plot (plot 2) and the shrub-grass plot (plot 3) , which are representative of different stages of the transition (mixed shrub and grass) to the shrub end-member (plot 4).

Figure 3. Experimental design of each study site comprising:

(i) Instrumented plot (10 x 30m) with 15 mini-flumes, mini-samplers and a supercritical flume (with pump auto-sampler to collect samples, measure flow depth and rainfall)

(ii) 5 x 30 m characterisation areas either side of the instrumented plot consisting of broad-scale sampling points and fine-scale nested sampling.

Figure 4. The instrumental set up which is identical at each plot, consisting of gutters at the base of the plot which channels runoff from the plot into a supercritical, instrumented with a bubbler module attached to the auto-sampler (left, the shrub-grass plot). From the super-critical flume, runoff is channelled down a pipe to a stock tank (right, the shrub plot) where all water, sediment and nutrients exported from the plot are collected.

Figure 5. Soil-moisture dynamics for 2005 and 2006. Boxes encompass the upper and lower quartiles of soil-moisture measurements whiskers show the 10th and 90th percentiles for bare, grass and/or shrub sampling points (90 sampling points per plot).

Figure 6. The range at which soil-moisture content is autocorrelated and the nugget variance through time.

Figure 7. Relationships between *ER* (event rainfall) and *RC* (runoff coefficient), *I* (maximum rainfall intensity) and *RC,* and I_5 (maximum 5-minute rainfall intensity) and *RC*. Error bars indicate potential error in runoff coefficients due to errors inherent in *Q* calculations. Dotted lines are linear trend lines between the runoff coefficient and rainfall characteristics.

Figure 8. Relationships between Q_m (maximum discharge) and *RC* (runoff coefficient), *I* (maximum rainfall intensity) and *RC,* and I_5 (maximum 5-minute rainfall intensity) and *RC*. Error bars indicate the potential error in runoff coefficients due to errors inherent in *Q* calculations. Dotted lines are linear trend lines between the runoff coefficient and rainfall characteristics.

Figure 9. Relationships between Q_t (total discharge) and *RC* (runoff coefficient), *I* (maximum rainfall intensity) and *RC,* and I_5 (maximum 5-minute rainfall intensity) and *RC*. Error bars indicate potential error in runoff coefficients due to errors inherent in *Q* calculations. Dashed lines are linear trend lines between the runoff coefficient and rainfall characteristics.

Figure 10. Modelled total runoff at each plot for different amounts of event rainfall (ER) (mm) at each plot. Lines are for visual guidance only. Note that above ER = 11, the shrub-grass plot produced more runoff than the shrub plot.

Figure 11. Relationship between sediment yield and (a) event rainfall (*ER*), (b) *I* (maximum rainfall intensity), (c) I_5 (maximum 5-minute rainfall intensity), (d) Q_m (maximum discharge) and (e) Q_t (total discharge). Error bars show potential error related to uncertainty in flow monitoring. Tables adjacent to each scatter plot present the slope of the regression, the R^2 and the significance value of the regression.

Figure 12. Particle-size distribution of eroded sediment for single runoff events monitored over plots 1 to 4.

Figure 13. Relationship between event sediment yield and D_{50} for each plot.

Figure 14. Enrichment ratios for each size fraction of eroded sediment. An enrichment ratio >1 indicates enrichment of sediment compared to the matrix soil, and enrichment ratios <1 indicate depletion.

Figure 15. Examples of the particle-size characteristics (sand, silt and clay) of sediment for events monitored over each plot. Rainfall intensities throughout the events, the hydrograph and flux of sediment are also shown.

Table 1. Characteristics of the study sites.

Plot	*Vegetation characteristics*				*Soil characteristics*			
	% vegetation cover	% grass cover	% shrub cover	Range of spatial autocorrelation (m)	% pebbles	% sand	% silt	% clay
Grass	45.5	45.5	0	0.7	27.8	50.8	18.8	2.6
Grass-shrub	43.0	38.6	4.4	0.7	20.8	56.2	20.2	2.8
Shrub-grass	26.2	14.3	11.9	1.0	48.8	32.6	17.1	1.5
Shrub	23.3	1.0	22.3	0.8	34.0	43.8	20.0	2.2

Table 2. Characteristics of monitored runoff events. Hydrographs of the events highlighted in bold are discussed in the text.

Plot	Date	Event rain (mm)	Max rainfall intensity (mm hr^{-1})	Time to runoff initiation (mins)	Rain prior to runoff initiation (mm)	RC	Total Q (litres)	Peak Q (l min^{-1})	Antecedent soil moisture prior to event (%)
1	21/08/2005	22.50	72.97	42	14.29	0.03	185.51	15.96	6.33
	07/09/2005	47.92	211.41	2	1.06	0.37	5275.22	288.77	7.65
	28/09/2005	6.89	63.64	16	5.83	0.02	37.85	8.71	4.47
	29/09/2005	5.33	50.49	7	2.52	0.08	124.13	20.12	20.04
	05/07/2006	12.94	69.33	3	3.70	0.07	276.64	35.24	6.02
	28/07/2006	10.41	45.72	4	1.02	0.06	177.33	10.57	11.31
	04/08/2006	5.08	45.72	9	3.56	0.02	26.58	5.09	13.45
	11/08/2006	10.92	60.96	4	1.02				10.25
	15/08/2006	7.11	45.72		0.00	0.07	141.87	74.41	
	23/08/2006	6.35	45.72	4	0.51	0.06	113.49	6.95	
	29/08/2006	23.11	213.36	5	0.51	0.41	2820.30	280.85	8.13
	07/09/2006	13.72	91.44	3	1.27	0.35	1425.75	150.05	14.06
2	07/09/2005	26.20	90.00	55	4.10	0.29	2294.44	196.69	8.39
	31/07/2006	5.59	30.48	10	3.56	0.05	82.92	9.34	16.44
	01/08/2006	9.40	60.96	10	2.79	0.16	464.36	49.52	19.32
	11/08/2006	11.43	60.96	15	7.87	0.04	149.26	20.69	10.56
	15/08/2006	9.40	60.96	8	3.30	0.14	391.39	47.85	
	29/08/2006	20.57	91.44	10	2.29	0.16	995.05	102.07	8.27
	07/09/2006	14.99	76.20	4	3.05	0.28	1260.39	105.18	13.73
3	28/09/2005	11.40	48.00	10	5.10	0.11	363.08	51.07	3.65
	29/09/2005	5.00	48.00	9	3.80	0.08	122.13	31.66	18.15
	05/07/2006	8.89	60.96	10	3.56	0.02	66.01	7.48	5.29
	28/07/2006	11.68	45.72	15	5.08	0.11	379.58	48.13	12.25
	31/07/2006	12.45	76.20	4	1.02	0.48	1798.88	223.80	15.51
	01/08/2006	14.48	106.68	5	2.03	0.47	2029.93	303.11	
	11/08/2006	9.40	60.96	8	3.56	0.23	637.04	114.36	
	23/08/2006	8.64	60.96	8	3.30				
	29/08/2006	7.37	60.96	9	2.54	0.25	567.72	95.55	9.04
	07/09/2006	24.38	91.44	10	2.29	0.90	6549.66	479.08	11.83
4	07/09/2005	14.10	108.00	6	2.60	0.51	2174.09	253.68	3.93
	28/09/2005	6.80	48.00	12	4.30				3.79
	29/09/2005	5.10	48.00	5	1.90	0.29	443.33	47.76	18.77
	05/07/2006	17.02	91.44	3	0.76	0.43	2174.09	157.90	5.77
	28/07/2006 a	14.73	76.20	4	0.76	0.34	1503.86	132.91	10.21
	28/07/2006 b	7.37	30.48	18	2.03	0.20	452.29	43.08	
	29/07/2006	5.84	30.48	24	2.54	0.11	199.20	14.94	
	31/07/2006	9.40	45.72	7	1.02	0.31	886.66	64.02	14.53
	01/08/2006	15.49	76.20	10	0.76	0.47	2174.09	99.40	17.21
	04/08/2006	3.56	45.72	2	0.51	0.12	126.55	17.16	16.50
	11/08/2006	7.11	60.96	6	2.00	0.21	450.42	53.04	10.72
	23/08/2006	9.91	60.96	11	2.54	0.47	1386.74	160.65	
	29/08/2006	37.08	106.68	6	1.78	0.57	6366.17	245.52	9.03
	02/09/2006	9.65	30.48	33	4.06	0.02	60.73	12.85	12.30

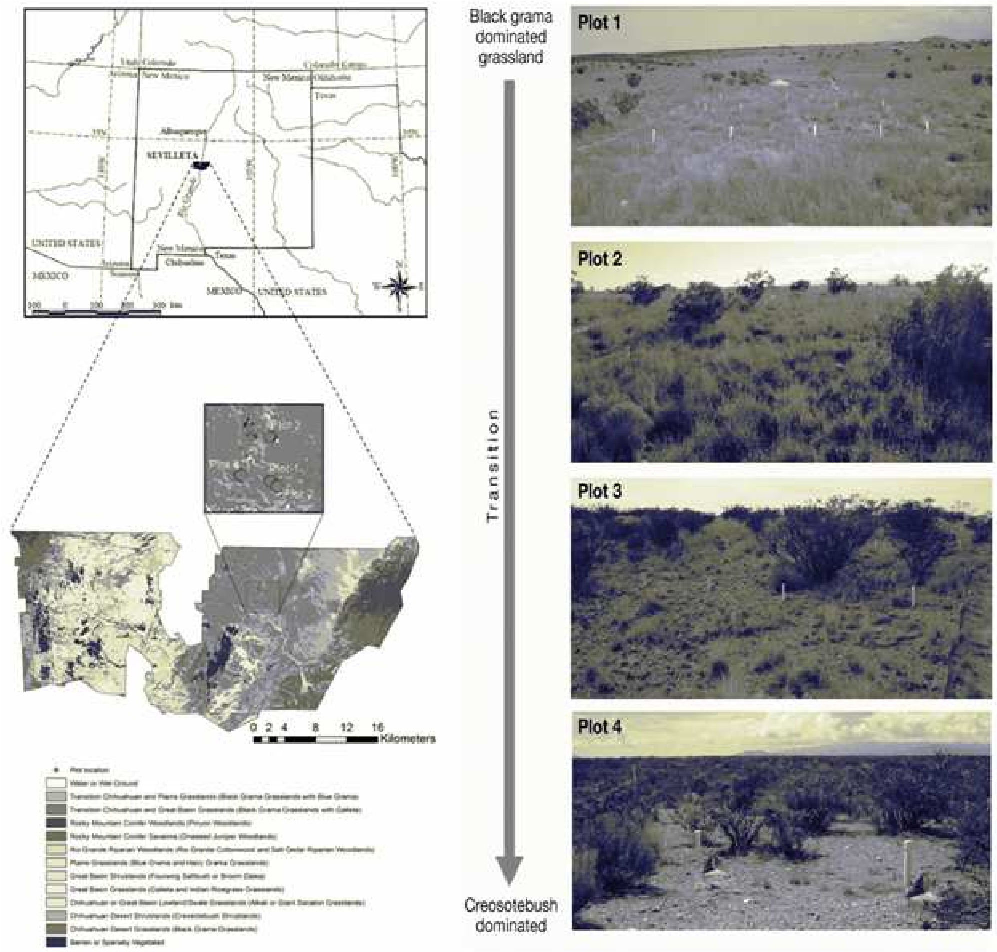

Location of the Sevilleta National Wildlife Refuge (SNWR) in the south-western USA and the location of the four study sites within the SNWR (grass = plot 1, grass-shrub = plot 2, shrub-grass = plot 3 and shrub = plot 4).
105x101mm (150 x 150 DPI)

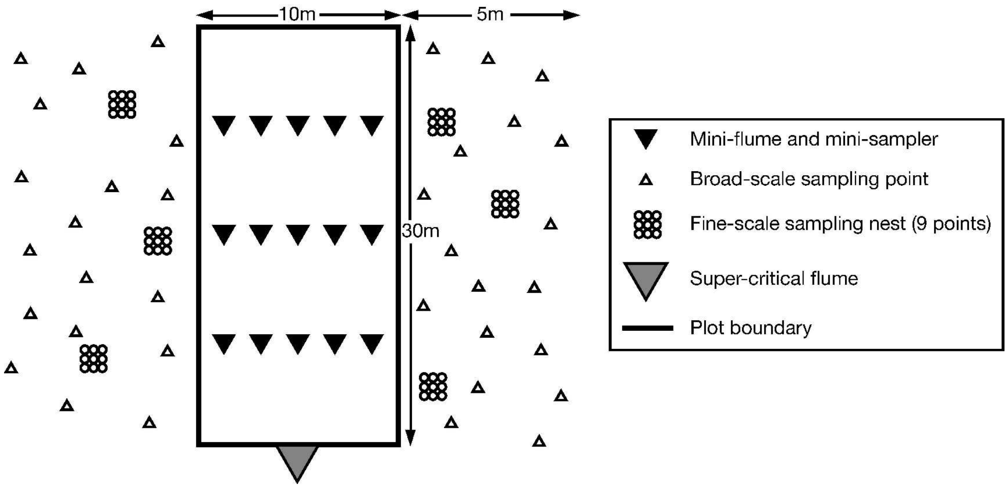

Experimental design of each study site comprising:
(i) Instrumented plot (10 x 30m) with 15 mini-flumes, mini-samplers and a supercritical flume (with pump auto-sampler to collect samples, measure flow depth and rainfall)
(ii) 5 x 30 m characterisation areas either side of the instrumented plot consisting of broad-scale sampling points and fine-scale nested sampling.

145x69mm (600 x 600 DPI)

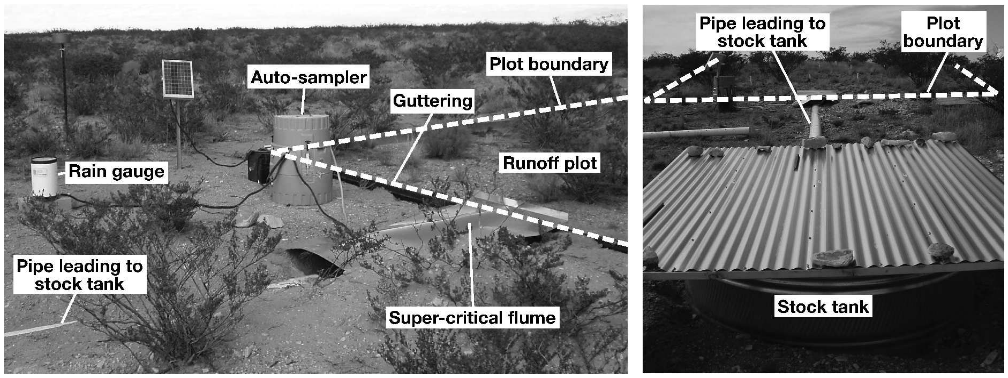

The instrumental set up which is identical at each plot, consisting of gutters at the base of the plot which channels runoff from the plot into a supercritical, instrumented with a bubbler module attached to the auto-sampler (left, plot 3). From the super-critical flume, runoff is channelled down a pipe to a stock tank (right, plot 4) where all water, sediment and nutrients exported from the plot are collected.
158x58mm (600 x 600 DPI)

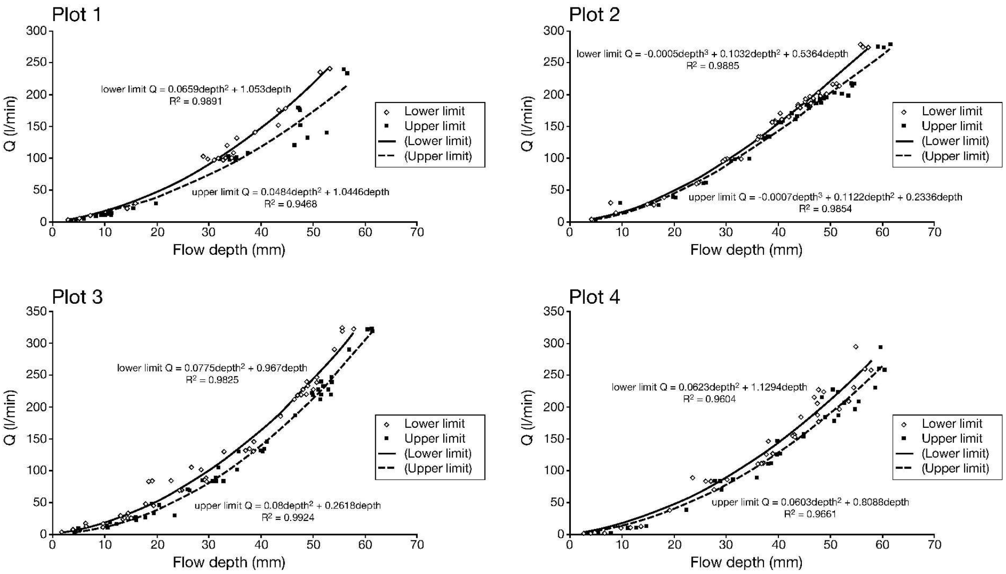

d/Q calibration curves for all runoff plots. Curves plotted for the upper (dashed line) and lower (solid line) limits of d for values of Q at the 95% confidence level. Red triangles mark the lower-limit depth measurements for Q and blue triangles mark the upper limit depth measurements for Q.
158x90mm (600 x 600 DPI)

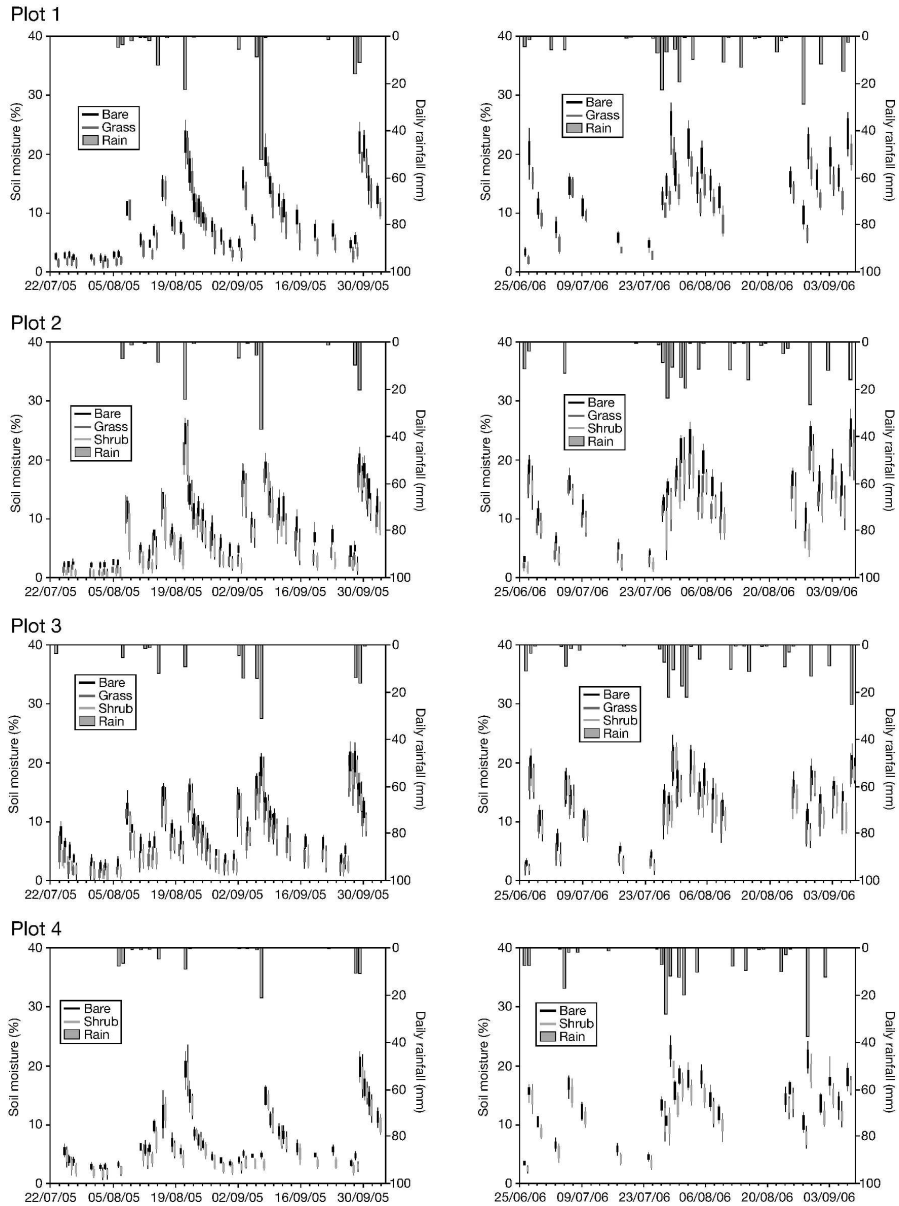

Soil-moisture dynamics for 2005 and 2006. Boxes encompass the upper and lower quartiles of soil-moisture measurements whiskers show the 10th and 90th percentiles for bare, grass and/or shrub sampling points (90 sampling points per plot).
148x200mm (600 x 600 DPI)

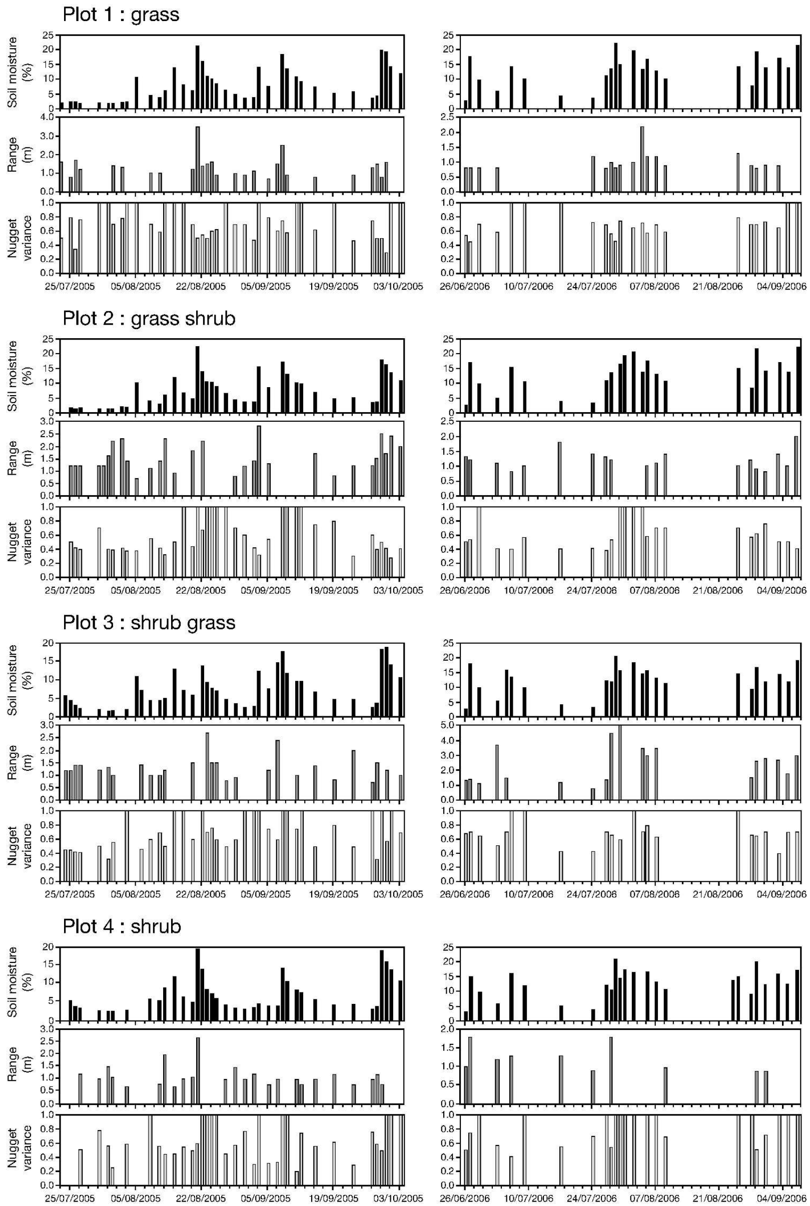

The range at which soil-moisture content is autocorrelated and the nugget variance through time.
127x190mm (600 x 600 DPI)

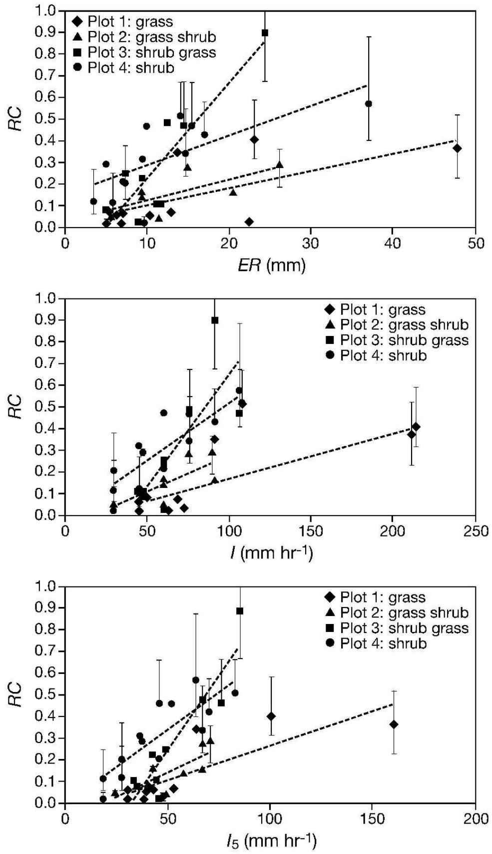

	Equation describing relationship	R^2	*p*
Plot 1	$RC = 0.0081ER - 0.0194$	0.45	0.024
Plot 2	$RC = 0.0097ER - 0.0259$	0.51	0.074
Plot 3	$RC = 0.0440ER - 0.2207$	0.77	0.002
Plot 4	$RC = 0.0139ER - 0.1448$	0.49	0.008
Plot 1	$RC = 0.0021I - 0.0451$	0.77	<0.0005
Plot 2	$RC = 0.0034I - 0.0670$	0.52	0.068
Plot 3	$RC = 0.0105I - 0.4055$	0.63	0.011
Plot 4	$RC = 0.0054I - 0.0245$	0.75	<0.0005
Plot 1	$RC = 0.0032I_5 - 0.0514$	0.67	0.002
Plot 2	$RC = 0.0045I_5 - 0.0829$	0.59	0.044
Plot 3	$RC = 0.0139I_5 - 0.4442$	0.85	<0.0005
Plot 4	$RC = 0.0070I_5 - 0.0047$	0.70	<0.0005

Relationships between ER (event rainfall) and RC (runoff coefficient), I (maximum rainfall intensity) and RC, and I_5 (maximum 5-minute rainfall intensity) and RC. Error bars indicate potential error in runoff coefficients due to errors inherent in Q calculations. Dotted lines are linear trend lines between the runoff coefficient and rainfall characteristics.
159x141mm (600 x 600 DPI)

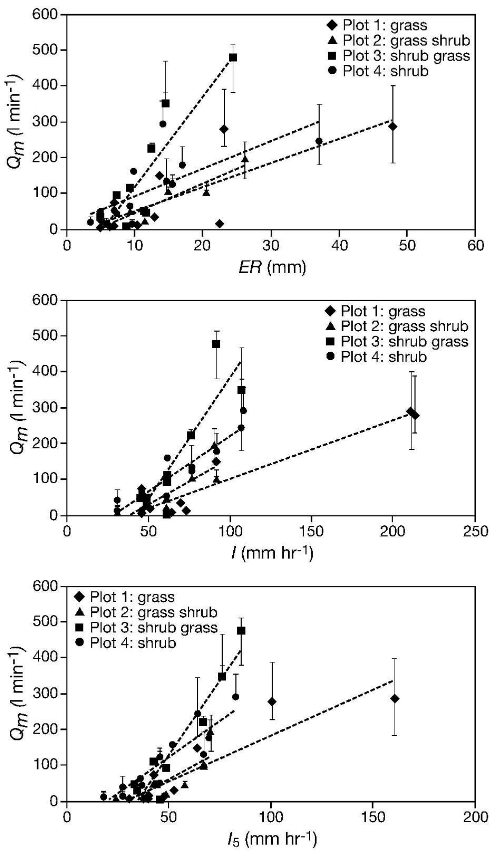

	Equation describing relationship	R^2	p
Plot 1	$Q_m = 6.7177ER - 17.029$	0.61	0.004
Plot 2	$Q_m = 8.3394ER - 41.175$	0.88	0.002
Plot 3	$Q_m = 25.712ER - 144.46$	0.77	0.002
Plot 4	$Q_m = 7.6694ER - 0.5225$	0.52	0.005
Plot 1	$Q_m = 1.6330I - 60.332$	0.91	<0.0005
Plot 2	$Q_m = 2.5550I - 96.011$	0.69	0.021
Plot 3	$Q_m = 6.8861I - 302.60$	0.79	0.001
Plot 4	$Q_m = 3.1277I - 88.192$	0.88	<0.0005
Plot 1	$Q_m = 2.5605I_5 - 69.135$	0.84	<0.0005
Plot 2	$Q_m = 3.1129I_5 - 92.476$	0.64	0.030
Plot 3	$Q_m = 8.3574I_5 - 288.68$	0.90	<0.0005
Plot 4	$Q_m = 4.0819I_5 - 79.015$	0.85	<0.0005

Relationships between Q_m (maximum discharge) and RC (runoff coefficient), I (maximum rainfall intensity) and RC, and I_5 (maximum 5-minute rainfall intensity) and RC. Error bars indicate the potential error in runoff coefficients due to errors inherent in Q calculations. Dotted lines are linear trend lines between the runoff coefficient and rainfall characteristics.
160x141mm (600 x 600 DPI)

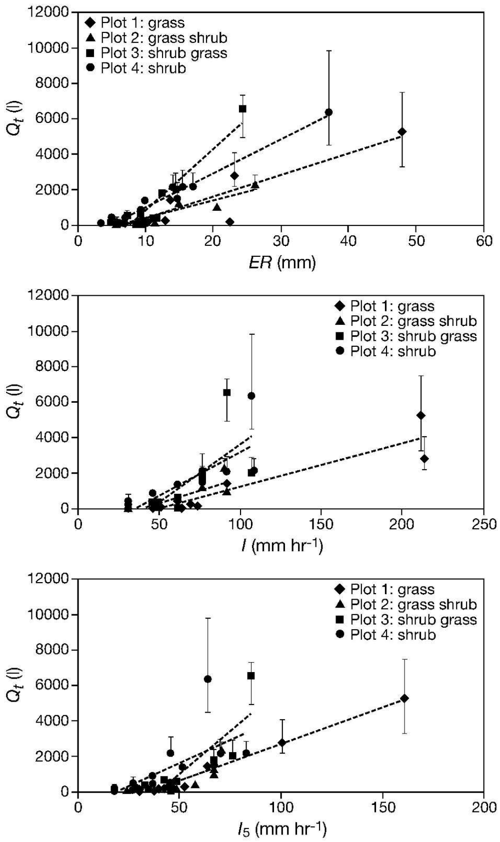

	Equation describing relationship	R^2	p
Plot 1	$Q_t = 119.51ER - 789.17$	0.84	0.002
Plot 2	$Q_t = 99.448ER - 580.83$	0.84	0.040
Plot 3	$Q_t = 346.86ER - 2658.0$	0.87	<0.0005
Plot 4	$Q_t = 190.96ER - 881.57$	0.95	<0.0005
Plot 1	$Q_t = 24.308I - 1147.4$	0.86	<0.0005
Plot 2	$Q_t = 29.3861I - 1171.9$	0.61	0.036
Plot 3	$Q_t = 67.217I - 3082.6$	0.47	0.041
Plot 4	$Q_t = 49.081I - 1647.8$	0.64	0.001
Plot 1	$Q_t = 41.169I_5 - 1517.1$	0.98	<0.0005
Plot 2	$Q_t = 32.205I_5 - 1153.0$	0.59	0.043
Plot 3	$Q_t = 94.748I_5 - 3646.9$	0.72	0.003
Plot 4	$Q_t = 51.443I_5 - 929.15$	0.40	0.021

Relationships between Q_t (total discharge) and RC (runoff coefficient), I (maximum rainfall intensity) and RC, and I_5 (maximum 5-minute rainfall intensity) and RC. Error bars indicate potential error in runoff coefficients due to errors inherent in Q calculations. Dashed lines are linear trend lines between the runoff coefficient and rainfall characteristics.
161x141mm (600 x 600 DPI)

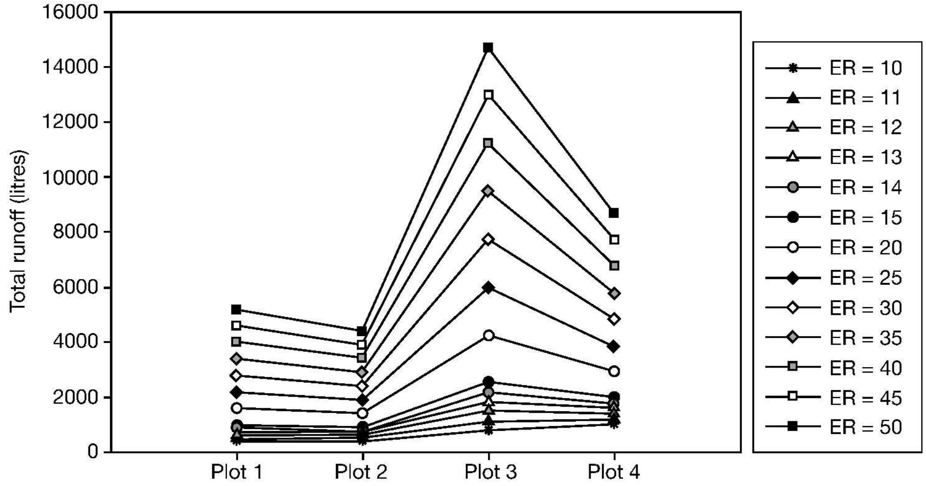

Modelled total runoff at each plot for different amounts of event rainfall (mm) (ER) at each plot. Lines are for visual guidance only. Note that above ER = 11, plot 3 produced more runoff than plot 4.
136x65mm (600 x 600 DPI)

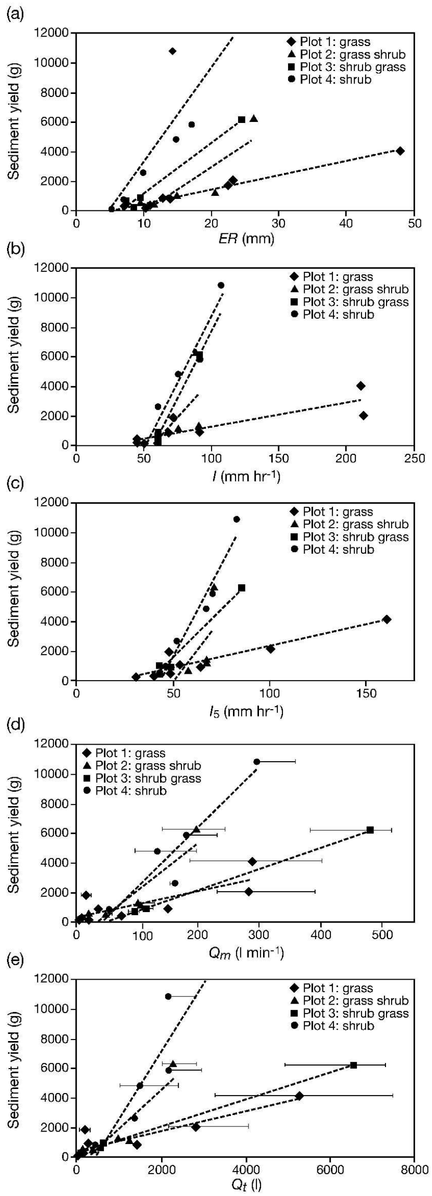

		Equation describing relationship	R^2	*p*
(a)	Plot 1	$SY = 96.97\,ER - 448.94$	0.98	0.000
(a)	Plot 2	$SY = 303.6\,ER - 3074.5$	0.74	0.063
(a)	Plot 3	$SY = 344.97\,ER - 2273.4$	0.98	0.008
(a)	Plot 4	$SY = 651.23\,ER - 3215.3$	0.47	0.204
(b)	Plot 1	$SY = 16.656\,I - 417.54$	0.75	0.001
(b)	Plot 2	$SY = 103.78\,I - 5937.7$	0.40	0.250
(b)	Plot 3	$SY = 181.86\,I - 10452$	0.99	0.004
(b)	Plot 4	$SY = 180.79\,I - 9401.5$	0.93	0.008
(c)	Plot 1	$SY = 29.971\,I_5 - 786.77$	0.88	0.000
(c)	Plot 2	$SY = 171.2\,I_5 - 8728.8$	0.40	0.256
(c)	Plot 3	$SY = 134.11\,I_5 - 5337.6$	0.98	0.011
(c)	Plot 4	$SY = 249.38\,I_5 - 10862$	0.95	0.006
(d)	Plot 1	$SY = 8.9886\,Q_m + 295.14$	0.62	0.120
(d)	Plot 2	$SY = 32.696\,Q_m - 1149.5$	0.82	0.033
(d)	Plot 3	$SY = 14.337\,Q_m - 693.19$	1.00	0.008
(d)	Plot 4	$SY = 41.079\,Q_m - 1762.8$	0.88	0.017
(e)	Plot 1	$SY = 0.6621\,Q_t + 406.01$	0.82	0.001
(e)	Plot 2	$SY = 2.6183\,Q_t - 725.48$	0.82	0.034
(e)	Plot 3	$SY = 0.9026\,Q_t + 266.5$	1.00	0.013
(e)	Plot 4	$SY = 4.5451\,Q_t - 2016.6$	0.72	0.070

Relationship between sediment yield and (a) ER (event rainfall), (b) I (maximum rainfall intensity), (c) I_5 (maximum 5-minute rainfall intensity), (d) Q_m (maximum discharge) and (e) Q_t (total runoff). Error bars show potential error related to uncertainty in flow monitoring. Tables adjacent to each scatter plot present the slope of the regression, the R^2 and the significance value of the regression.
143x199mm (600 x 600 DPI)

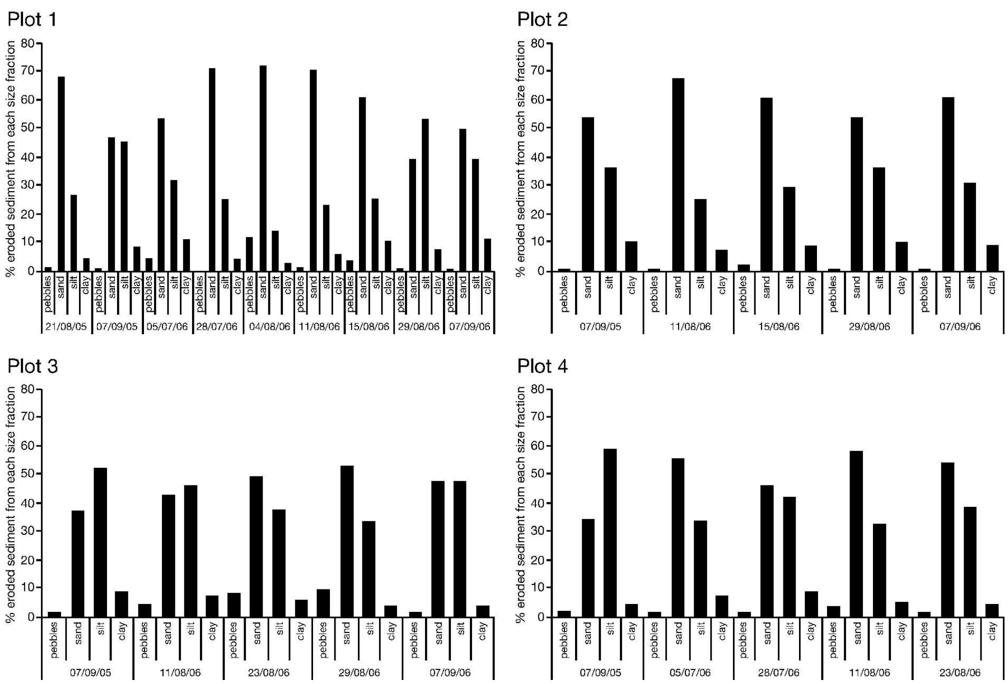

Particle-size distribution of eroded sediment for single runoff events monitored over plots 1 to 4.
160x107mm (600 x 600 DPI)

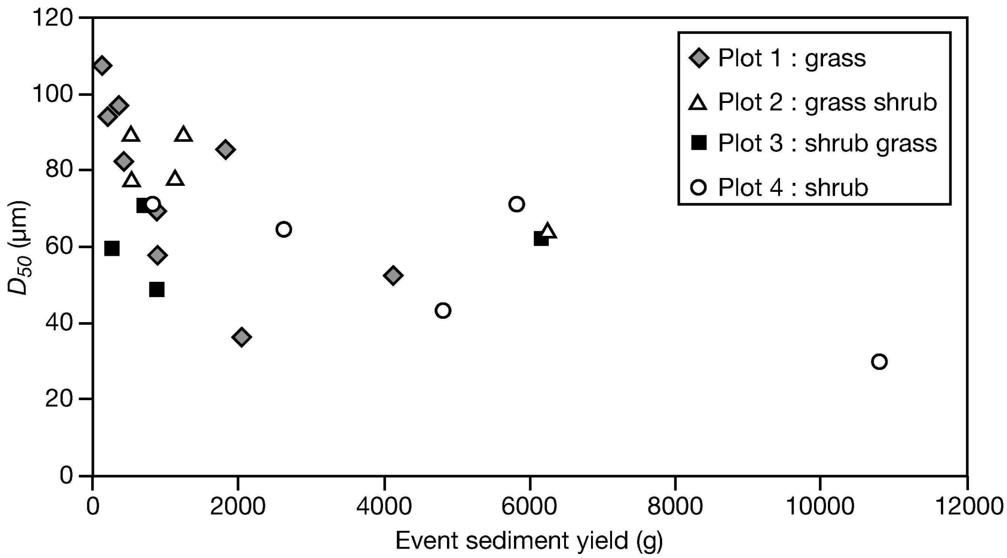

Relationship between event sediment yield and D_{50} for each plot.
113x62mm (600 x 600 DPI)

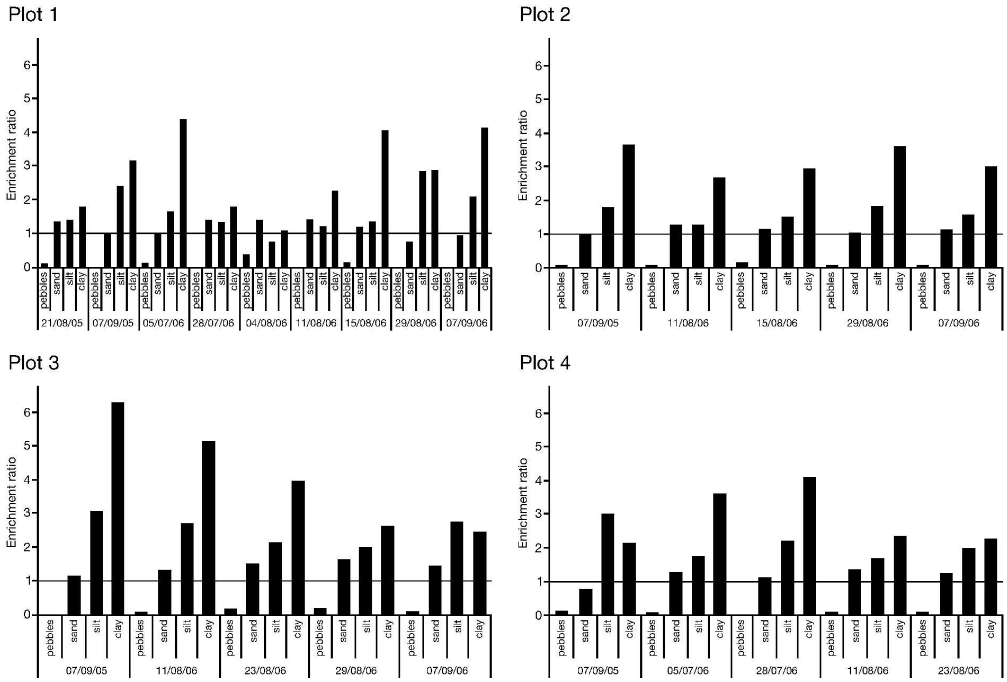

Enrichment ratios for each size fraction of eroded sediment. An enrichment ratio >1 indicates enrichment of sediment compared to the matrix soil, and enrichment ratios <1 indicate depletion.
159x107mm (600 x 600 DPI)

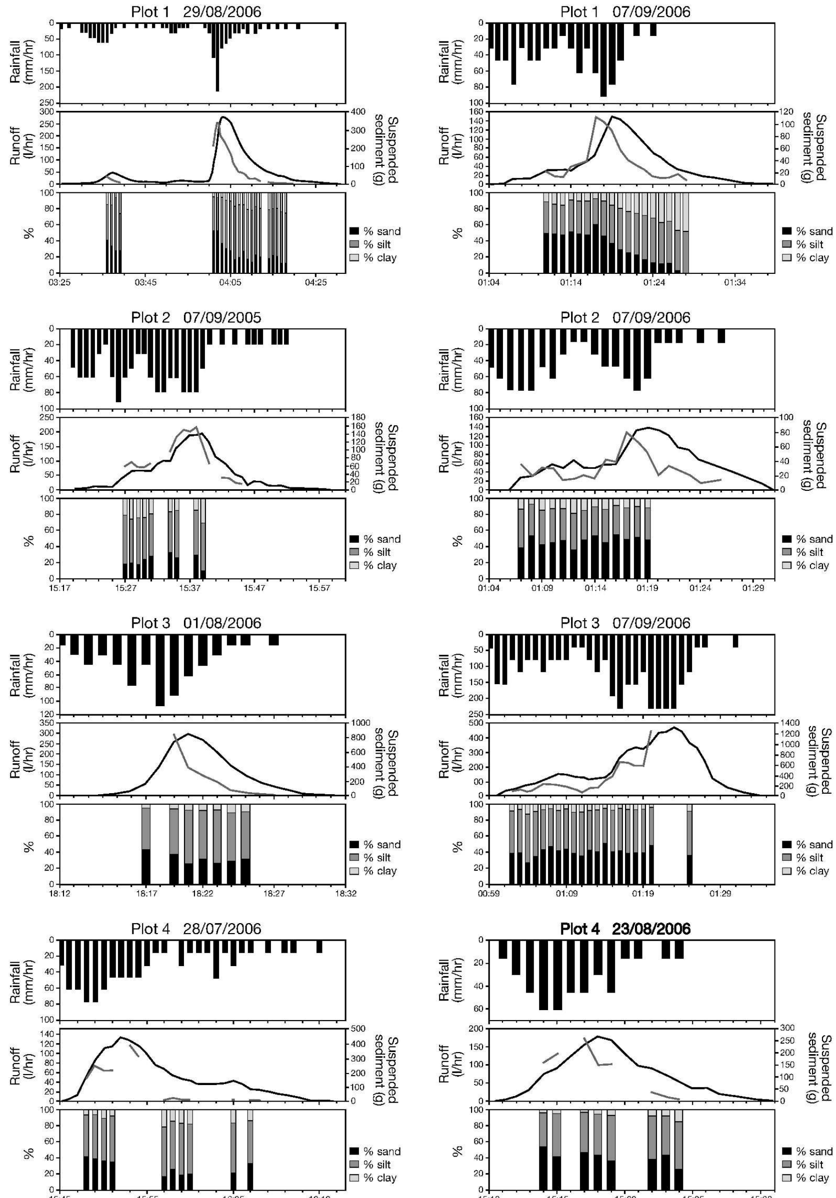

Examples of the particle-size characteristics (sand, silt and clay) of sediment for events monitored over each plot. Rainfall intensities throughout the events, the hydrograph and flux of sediment are also shown.
133x193mm (600 x 600 DPI)